Towards A Model-based Prognostics Methodology for Electrolytic Capacitors: A Case Study Based on Electrical Overstress Accelerated Aging

José R. Celaya[1], Chetan S. Kulkarni[2], Gautam Biswas[3], and Kai Goebel[4]

[1] *SGT Inc. NASA Ames Research Center, Moffett Field, CA, 94035, USA*
jose.r.celaya@nasa.gov

[2, 3] *Vanderbilt University, Nashville, TN, 37235, USA*
chetan.kulkarni@vanderbilt.edu
biswas@eecsmail.vuse.vanderbilt.edu

[5] *NASA Ames Research Center, Moffett Field, CA, 94035, USA*
kai.goebel@nasa.gov

ABSTRACT

A remaining useful life prediction methodology for electrolytic capacitors is presented. This methodology is based on the Kalman filter framework and an empirical degradation model. Electrolytic capacitors are used in several applications ranging from power supplies on critical avionics equipment to power drivers for electro-mechanical actuators. These devices are known for their comparatively low reliability and given their criticality in electronics subsystems they are a good candidate for component level prognostics and health management. Prognostics provides a way to assess remaining useful life of a capacitor based on its current state of health and its anticipated future usage and operational conditions. We present here also, experimental results of an accelerated aging test under electrical stresses. The data obtained in this test form the basis for a remaining life prediction algorithm where a model of the degradation process is suggested. This preliminary remaining life prediction algorithm serves as a demonstration of how prognostics methodologies could be used for electrolytic capacitors. In addition, the use degradation progression data from accelerated aging, provides an avenue for validation of applications of the Kalman filter based prognostics methods typically used for remaining useful life predictions in other applications.

1. INTRODUCTION

This paper proposes the use of a model based prognostics approach for electrolytic capacitors. Electrolytic capacitors have become critical components in electronics systems in aeronautics and other domains. This type of capacitors are known for their low reliability and frequent breakdown in critical systems like power supplies of avionics equipment and electrical drivers of electro-mechanical actuators of control surfaces. The field of prognostics for electronics components is concerned with the prediction of remaining useful life (RUL) of components and systems. In particular, it focuses on condition-based health assessment by estimating the current state of health. Furthermore, it leverages the knowledge of the device physics and degradation physics to predict remaining useful life as a function of current state of health and anticipated operational and environmental conditions.

1.1. Motivation

The development of prognostics methodologies for the electronics field has become more important as more electrical systems are being used to replace traditional systems in several applications in fields like aeronautics, maritime, and automotive. The development of prognostics methods for electronics presents several challenges due to great variety of components used in a system, a continuous development of new electronics technologies, and a general lack of understanding of how electronics fail. Traditional reliability techniques in electronics tend to focus on understanding the time to failure for a batch of components of the same type. Just until recently, there has been a push to understand, in more depth, how a fault progresses as a function of usage, namely,

loading and environmental conditions. Furthermore, just until recently, it was believed that there were no precursor of failure indications for electronics systems. That is now understood to be incorrect, since electronics systems, similar to mechanical systems, undergo a measurable wear process from which one can derive features that can be used to provide early warnings to failure. These failures can be detected before they happen and one can potentially predict the remaining useful life as a function of future usage and environmental conditions.

Avionics systems in on-board autonomous aircraft perform critical functions greatly escalating the ramification of an in-flight malfunction (Bhatti & Ochieng, 2007; Kulkarni et al., 2009). These systems combine physical processes, computational hardware and software; and present unique challenges for fault diagnosis. A systematic analysis of these conditions is very important for analysis of aircraft safety and also to avoid catastrophic failures during flight.

Power supplies are critical components of modern avionics systems. Degradations and faults of the DC-DC converter unit propagate to the GPS (global positioning system) and navigation subsystems affecting the overall operation. Capacitors and MOSFETs (metal oxide field effect transistor) are the two major components, which cause degradations and failures in DC-DC converters (Kulkarni, Biswas, Bharadwaj, & Kim, 2010). Some of the more prevalent fault effects, such as a ripple voltage surge at the power supply output can cause glitches in the GPS position and velocity output, and this in turn, if not corrected can propagate and distort the navigation solution.

Capacitors are used as filtering elements on power electronics systems. Electrical power drivers for motors require capacitors to filter the rail voltage for the H-bridges that provide bidirectional current flow to the windings of electrical motors. These capacitors help to ensure that the heavy dynamic loads generated by the motors do not perturb the upstream power distribution system. Electrical motors are an essential element in electro-mechanical actuators systems that are being used to replace hydro-mechanical actuation in control surfaces of future generation aircrafts.

1.2. Previous work

In earlier work (Kulkarni, Biswas, Koutsoukos, Goebel, & Celaya, 2010b), we studied the degradation of capacitors under nominal operation. There, work capacitors were used in a DC-DC converter and their degradation was monitored over an extended period of time. The capacitors were characterized every 100-120 hours of operation to capture degradation data for ESR and capacitance. The data collected over the period of about 4500 hours of operation were then mapped against an Arrhenius inspired ESR degradation model (Kulkarni, Biswas, Koutsoukos, Goebel, & Celaya, 2010a).

In following experimental work, we studied accelerated degradation in capacitors (Kulkarni, Biswas, Koutsoukos, Celaya, & Goebel, 2010). In that experiment the capacitors were subjected to high charging/discharging cycles at a constant frequency and their degradation progress was monitored. A preliminary approach to remaining useful life prediction of electrolytic capacitors was presented in (Celaya et al., 2011b). This paper here builds upon the work presented in the preliminary remaining useful life prediction in (Celaya et al., 2011a) and experimental studies done in (Celaya et al., 2012).

1.3. Other related work and current art in capacitor prognostics

The output filter capacitor has been identified as one of the elements of a switched mode power supply that fails more frequently and has a critical impact on performance (Goodman et al., 2007; Judkins et al., 2007; Orsagh et al., 2005). A prognostics and health management approach for power supplies of avionics systems is presented in (Orsagh et al., 2005). Results from accelerated aging of the complete supply were presented and discussed in terms of output capacitor and power MOSFET failures; but there is no modeling of the degradation process or RUL prediction for the power supply. Other approaches for prognostics for switched mode power supplies are presented in Goodman et al. (2007) and Judkins et al. (2007). The output ripple voltage and leakage current are presented as a function of time and degradation of the capacitor, but no details were presented regarding the modeling of the degradation process and there were no technical details on fault detection and RUL prediction algorithms.

A health management approach for multilayer ceramic capacitors is presented in Nie et al. (2007). This approach focuses on the temperature-humidity bias accelerated test to replicate failures. A method based on Mahalanobis distance is used to detect abnormalities in the test data; there is no prediction of RUL. A data driven prognostics algorithm for multilayer ceramic capacitors is presented in Gu et al. (2008). This method uses data from accelerated aging test to detect potential failures and to make an estimation of time of failure.

2. PROGNOSTICS METHODOLOGY

The process followed in the proposed prognostics methodology is presented in the block diagram in Figure 1. It is based on a model-based prognostics framework using an time-dependent empirical degradation model build from accelerated aging tests.

Accelerated Aging: The methodology is based on results from an accelerated life test on real electrolytic capacitors. This test applies electrical overstress to commercial, off the

shelf capacitors, in order to observe and record the degradation process and identify performance conditions in the neighborhood of the failure criteria in a considerably reduced time frame. A total of 6 accelerated aging test devices are available for the development of the proposed methodology. Electrochemical-impedance spectroscopy (EIS) is used periodically during the accelerated aging test to characterize the frequency response of the capacitor's impedance. Several measurements are available through the aging time, including measurements at pristine condition and measurements after failure condition.

System Identification: A lumped-parameter model ($\mathcal{M}_1$) of the non-ideal capacitor impedance is assumed. This impedance model includes a capacitance element and an equivalent series resistance (ESR) parasitic element. The EIS measurements along with the impedance model structure are used in a systems identification setting to estimate the model parameters available throughout the aging test. This results in time-dependent capacitance and ESR measurements trajectories reflecting capacitor degradation.

Degradation Modeling: We present here an empirical degradation model that is based on the observed degradation process during the accelerated life test. The objective of the model is to generate a parametrized model of the time-dependent capacitance degradation as generated by the system identification step. A similar degradation model can be generated for ESR but not considered in this work.

Parameter Estimation: The parameters of the degradation model are estimated using nonlinear least-squares regression. The quality of the fit is good enough as to assume these parameters as static during the prognostics process.

Prognostics: A Bayesian framework is employed to estimate (track) the state of health of the capacitor based on measurement updates of key capacitor parameters. The Kalman filter algorithm is used to track the state of health and the degradation model is used to make predictions of remaining useful life once no further measurements are available.

3. ACCELERATED AGING EXPERIMENTS

Accelerated life test methods are often used in prognostics research as a way to assess the effects of the degradation process through time. It also allows for the identification and study of different failure mechanisms and their relationships with different observable signals and parameters. In the following section we present the accelerated aging methodology and an analysis of the degradation pattern induced by the aging. The work presented here is based on an accelerated electrical overstress. In the following subsections, we first present a brief description of the aging setup followed by an analysis of the observed degradation. The precursor to failure is also identified along with the physical processes that contribute to the degradation.

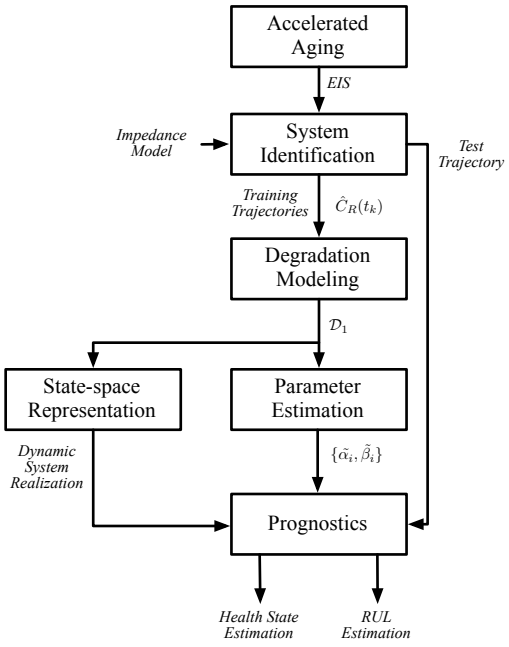

Figure 1. Methodology for capacitor prognostics.

3.1. Experimental Setup

Since the objective of this experiment is studying the effects of high voltage on degradation of the capacitors, the capacitors were subjected to high voltage stress through an external supply source using a specially developed hardware. The capacitors are stressed under high voltage conditions and specially developed hardware. The voltage overstress is applied to the capacitors as a square waveform in order to subject the capacitor to continuous charge and discharge cycles.

At the beginning of the accelerated aging, the capacitors charge and discharge simultaneously; as time progresses and the capacitors degrade, the charge and discharge times vary for each capacitor. Even though all the capacitors under test are subjected to similar operating conditions, their ESR and capacitance values change differently. We therefore monitor charging and discharging of each capacitor under test and measure the input and output voltages of the capacitor. Figure 2 shows the block diagram for the electrical overstress experiment. Additional details on the accelerated aging system are presented in (Kulkarni, Biswas, Koutsoukos, Celaya, & Goebel, 2010).

For this experiment six capacitors in a set were considered for the EOS experimental setup. Electrolytic capacitors of 2200μF capacitance, with a maximum rated voltage of $10V$, maximum current rating of $1A$ and maximum operating temperature of $105°C$ were used for the study. These were the recommended capacitors by the manufacturer for DC-DC

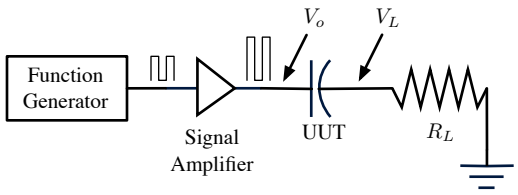

Figure 2. Block diagram of the experimental setup.

converters. The electrolytic capacitors under test were characterized in detail before the start of the experiment at room temperature.

The measurements were recorded every 8-10 hours of the total 180 plus hours of accelerated aging time to capture the rapid degradation phenomenon in the ESR and capacitance values. The ambient temperature for the experiment was controlled and kept at $25°C$. During each measurement the voltage source was shut down, capacitors were discharged completely and then the characterization procedure was carried out. This was done for all the six capacitors under test. For further details regarding the aging experiment results and analysis of the measured data refer to (Kulkarni, Biswas, Koutsoukos, Celaya, & Goebel, 2010; Celaya et al., 2011b).

3.2. Physical interpretation of the degradation process

There are several factors that cause electrolytic capacitors to fail. Continued degradation, i.e., gradual loss of functionality over a period of time results in the failure of the component. Complete loss of function is termed a *catastrophic* failure. Typically, this results in a short or open circuit in the capacitor. For capacitors, degradation results in a gradual increase in the equivalent series resistance and decrease in capacitance over time.

In this work, we study the degradation of electrolytic capacitors operating under high electrical stress, i.e., $V_{applied} \geq V_{rated}$. During the charging/discharging process the capacitors degrade over the period of time. A study of the literature indicated that the degradation could be primarily attributed to electrolyte evaporation, leakage current and increase in internal pressure due to gas released due to chemical reactions (IEC, 2007-03; MIL-C-62F, 2008; Kulkarni, Biswas, Koutsoukos, Goebel, & Celaya, 2010a). An ideal capacitor would offer no resistance to the flow of current at its leads. However, the electrolyte that fills the space between the plates and the electrodes produces a small equivalent internal series resistance. Fig. 3 shows the structure of an electrolytic capacitor in detail. The ESR dissipates some of the stored energy in the capacitor leading to increase in the internal temperature and thus causing electrolyte evaporation.

ESR and capacitance are the two main failure precursors that tipify the current health state of the device. ESR and capacitance values were calculated after characterizing the capacitors at regular intervals. As the devices degrade due to different failure mechanisms we can observe a decrease in the capacitance and an increase in the ESR.

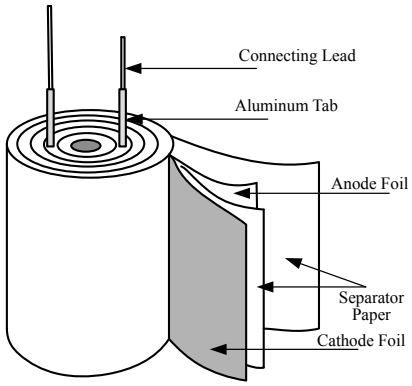

Figure 3. Electrolytic capacitor structure.

The literature on capacitor degradation shows a direct relationship between electrolyte decrease with increase in ESR and decrease in capacitance value of the capacitor (Kulkarni, Biswas, Koutsoukos, Goebel, & Celaya, 2010b). ESR increase implies greater dissipation, and, therefore, a slow decrease in the average output voltage at the capacitor leads.

ESR and capacitance values are estimated by using a system identification using a lump parameter model consistent of the capacitance and the ESR in series as shown in Figure 4. The frequency response of the capacitor impedance (measured with electro-impedance spectroscopy) is used for the parameter estimation. It should be noted that the lumped-parameter model used to estimate ESR and capacitance, is not the model to be used in the prognostics algorithm; it only allows us to estimate parameters which provide indications of the degradation process through time. Parameters such as ESR and capacitance are challenging to estimate from the *in-situ* measurements of voltage and current through the accelerated aging test.

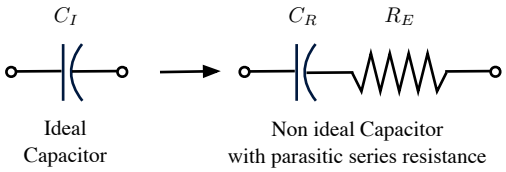

Figure 4. Lumped parameter model ($\mathcal{M}_1$) for a real capacitor.

3.3. System identification for real capacitor model

The ESR and capacitance values were estimated from the capacitor impedance frequency response measured using an SP-150 Biologic SAS electro-impedance spectroscopy instrument. A lumped parameter model consisting of a capacitor with a resistor in series was assumed to estimate the ESR and

capacitance.

The ideal capacitor has complex impedance $Z_I = 1/sC_I$ where C_I is the ideal capacitance value. The complex impedance of model $\mathcal{M}_1$ is given by

$$Z = R_E + \frac{1}{sC_R}, \tag{1}$$

where R_E is the equivalent series resistance and C_R is the real capacitance.

Electrochemical impedance spectroscopy measurements are available to characterize the electrical performance of the capacitor. Figure 5 shows Nyquist plots of the impedance measurements for capacitor $\#1$ at pristine condition and after accelerated aging at intervals of 71, 161 and 194 hours. The degradation can be observed as the Nyquist plot shifts to the right as a function of aging time due to increase in R_E. These measurement are then used to estimate the parameters of the impedance model $\mathcal{M}_1$ from eq. (1). The parameter estimation performed using the EIS instrument software (EC lab). This is basically and optimization problem using an aggregate of mean squared error as an objective function. The error is aggregated at different frequencies for which measurements are available. The optimization is set up to minimize the objective function by finding optimal values for ${C_R}^*$ and ${R_E}^*$.

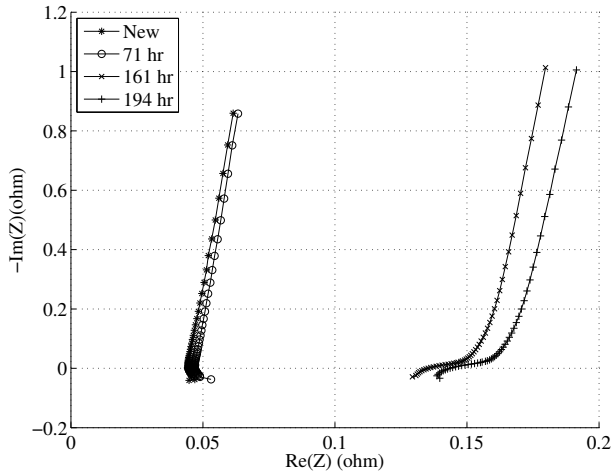

Figure 5. Electroimpedance measurements at different aging times.

This parameter estimation is performed every time an EIS measurement is taken resulting on values of C_R and R_E at different points in time through the aging of the components. The average pristine condition ESR value was measured to be $0.056\ m\Omega$ and average capacitance of $2123\ \mu$F individually for the set of capacitors under test.

Figure 6 shows percentage increase in the ESR value for all the six capacitors under test over the period of time. This value of ESR is calculated from the impedance measurements after characterizing the capacitors. Similarly, figure 7 shows the percentage decrease in the value of the capacitance as the capacitor degrades over the period under EOS test condition discussed. As per standards MIL-C-62F (2008), a capacitor is considered unhealthy if under electrical operation its ESR increases by $280 - 300\%$ of its initial value or the capacitance decreases by 20% below its pristine condition value. From the plots in Figure 6 we observe that for the time for which the experiments were conducted the average ESR value increased by $54\% - 55\%$ while over the same period of time, the average capacitance decreased by more than 20% (the threshold mark for a healthy capacitor) (see Figure 7). As a result, the percentage capacitance loss is selected as a precursor of failure variable to be used in the degradation model development presented next.

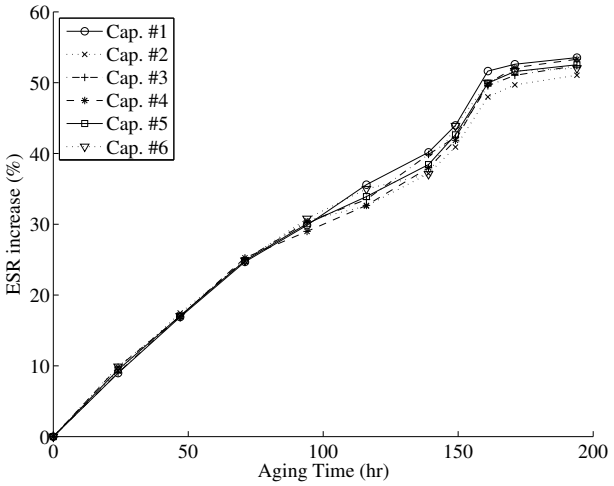

Figure 6. Degradation of capacitor performance, percentage ESR increase as a function of aging time.

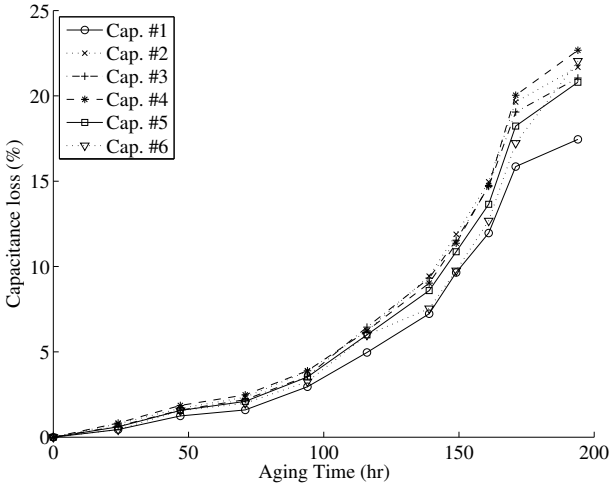

Figure 7. Degradation of capacitor performance, percentage capacitance loss as a function of aging time.

4. DEGRADATION MODELING FOR PROGNOSTICS

This sections presents the details of the degradation model development. A degradation model is an essential part of a model-based prognostics algorithm and it is typically application dependent. A model is formulated based on the empirical evidence of the degradation process time evolution from experiments presented in the previous section, particularly, capacitance loss as described by figure 7.

4.1. Nominal model

The non-ideal capacitor model $\mathcal{M}_1$ can be used as part of electronics circuits that make use of capacitors. An example is the low-pass filter implementation in figure 8. In this circuit, input voltage V_i is considered as the voltage to be filtered and the voltage across the capacitor (this includes R_E as well) is the output voltage V_o which is filtered. Let $v(t) = V_o(t)$ and $u(t) = V_i(t)$ in the low-pass system circuit with non-ideal capacitor shown in figure 8. A state-space realization ($\mathcal{M}_2$) of the dynamic system is given by

$$\dot{z}(t) = \frac{-1}{C_R(R+R_E)}z + \frac{1}{C_R(R+R_E)}u(t), \qquad (2)$$
$$v(t) = \left[1 - \frac{R_E}{R+R_E}\right]z + \frac{R_E}{R+R_E}u(t),$$

where $z(t) = V_C(t)$ is the state variable representing the capacitor voltage, C_R, R_E and R are system parameters. Furthermore, C_R and R_E are parameters that will change through time as the capacitor degrades.

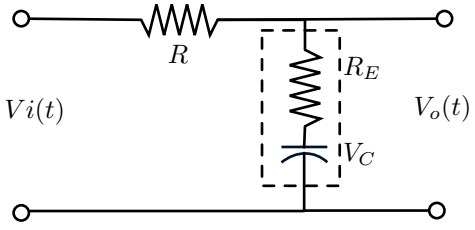

Figure 8. Low pass filter model ($\mathcal{M}_2$).

Model $\mathcal{M}_1$ describes the nominal dynamics of a low-pass filter with a non-ideal capacitor. This model by itself is not sufficient to implement a model-based prognostics algorithm since the degradation process as reflected on model parameters is not modeled. Degradation models describing the time evolution of R_E or C_R are needed in order to enhance $\mathcal{M}_1$ for model-based prognostics. Nevertheless, $\mathcal{M}_1$ is useful in this form for model-based fault detection and isolation which is not covered in this work.

4.2. Degradation model

The percentage loss in capacitance is used as a precursor of failure variable and it is used to build a model of the degradation process. This model relates aging time to the percentage loss in capacitance. Let C_l be the percentage loss of capacitance due to degradation as shown by figure 7. The following equation is a *degradation model* $\mathcal{D}$ of the capacitance parameter in the real capacitor model $\mathcal{M}_1$.

$$\mathcal{D}_1 : C_l(t) = e^{\alpha t} + \beta, \qquad (3)$$

where α and β are degradation model parameters that will be estimated from the experimental data of accelerated aging experiments.

In order to estimate the model parameters, five capacitors are used for estimation, and the remaining capacitor is used to test the prognostics algorithm. This results in six leave-one-out test cases for validation of the prognostics algorithm results. A nonlinear least-squares regression algorithm is used to estimate the model parameters. Table 1 presents definition of the test cases and the parameter estimation results. The estimate and 95% confidence interval is presented for parameters α and β. In addition, the error variance is included as a way to assess the quality of the fit.

Figure 9 shows the estimation results for test case T_6. The experimental data are presented together with results from the exponential fit function. It can be observed from the residuals that the estimation error increases with time. This is to be expected since the last data point measured for all the capacitors fall slightly off the concave exponential model.

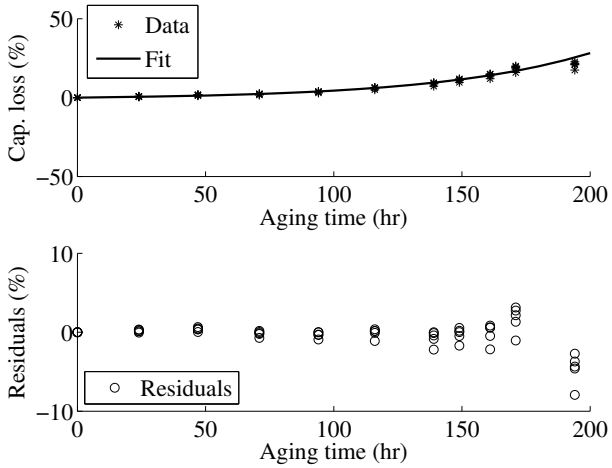

Figure 9. Estimation results for the empirical degradation model.

It should be noted that this degradation model with static parameters will be used in a Bayesian tracking framework. This will help to overcome the degradation model limitation to represent the behavior close to the failure threshold given the tracking framework ability to compensate the estimation as measurements become available.

Validation test	Test capacitor	Training capacitor	α (95% CI)	β (95% CI)	σ_v^2
T_2	#2	#1, #3–#6	**0.0162** (0.0160, 0.0164)	**-0.8398** (-1.1373, -0.5423)	1.8778
T_3	#3	#1, #2, #4–#6	**0.0162** (0.0160, 0.0164)	**-0.8287** (-1.1211, -0.5363)	1.9654
T_4	#4	#1–#3, #5, #6	**0.0161** (0.0159, 0.0162)	**-0.8217** (-1.1125, -0.5308)	1.8860
T_5	#5	#1–#4, #6	**0.0162** (0.0161, 0.0164)	**-0.7847** (-1.1134, -0.4560)	2.1041
T_6	#6	#1–#5	**0.0169** (0.0167, 0.0170)	**-1.0049** (-1.2646, -0.7453)	2.9812

Table 1. Degradation model parameter estimation results.

4.3. State-space realization for tracking

The estimated degradation model is used as part of a Bayesian tracking framework to be implemented using the Kalman filter technique. This method requires a state-space dynamic model relating the degradation level at time t_k to the degradation level at time t_{k-1}. The procedure to obtain a state-space model for $\mathcal{D}_1$ is as follows. The non-linear exponential behavior described in the model is represented as a first order differential equation which can represent the time evolution of $C_l(t)$. Then, the model is discretized in time in order to obtain a discrete-time state-space model $\mathcal{D}_2$.

From equation (3) we have that $C_l(t) = e^{\alpha t} + \beta$, taking the first derivative with respect to time and substituting $e^{\alpha t} = C_l(t) - \beta$ from eq. (3) we have

$$\dot{C}_l = \frac{dC_l(t)}{dt} = \alpha C_l(t) - \alpha\beta. \tag{4}$$

Taking the finite difference approximation for $\dot{C}_l$ with time interval Δt we have

$$\frac{C_l(t) - C_l(t-\Delta t)}{\Delta t} = \alpha C_l(t-\Delta t) - \alpha\beta, \text{ and}$$
$$C_l(t) = (1 + \alpha\Delta_t)C_l(t-\Delta t) - \alpha\beta\Delta_t.$$

Letting $t_k = t$ and $t_{k-1} = t - \Delta t$ we get the state-space model

$$C_l(t_k) = (1 + \alpha\Delta_k)C_l(t_{k-1}) - \alpha\beta\Delta_k. \tag{5}$$

This model can be used in a Bayesian tracking framework in order to continuously estimate the value of the loss in capacitance through time as measurement become available.

5. MODEL-BASED PROGNOSTICS FRAMEWORK

A model-based prognostics algorithm based on Kalman filter and a physics inspired empirical degradation model is presented. This algorithm is able to predict remaining useful life of the capacitor based on the accelerated degradation data from the experiments described in previous sections.

The methodology consists of the following three main steps and it is depicted in fig. 10.

1. State tracking (Kalman Filter): The capacitance loss C_l is defined as the state variable to be estimated and the degradation model is expressed as a discrete time dynamic model in order to estimate capacitance loss as new measurements become available. Direct measurements of the capacitance are assumed for the filter.

2. Health state forecasting: It is necessary to forecast the state variable once there are no more measurements available at time or RUL prediction t_p. This is done by evaluating the degradation model through time using the state estimate at time t_p as initial value.

3. Remaining life computation: RUL is computed as the time between time of prediction t_p and the time at which the forecasted state crosses the failure threshold value.

This process is repeated for different values of t_p through the life of the component under consideration.

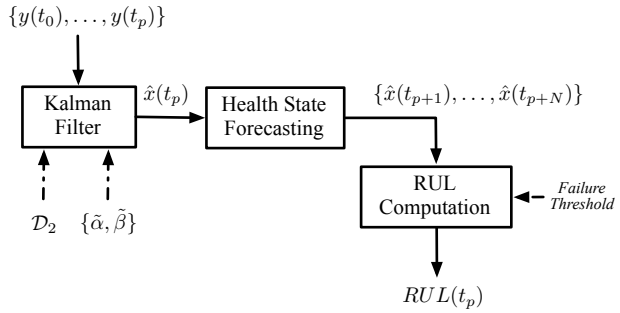

Figure 10. Model-based prognostics methodology

5.1. Kalman filter for state estimation

A state-space dynamic model is needed for the filtering. The state variable x_k at time t_k is defined as the percentage capacitance loss $C_l(k)$. Since the system measurements are percentage loss in capacitance as well, the output equation is given by $y_k = hx_k$, where the value of h is equal to one. The following system structure is used in the implementation of the filtering and the prediction using the Kalman filter.

$$\begin{aligned} x_k &= A_k x_{k-1} + B_k u + v, \\ y_k &= hx_k + w, \end{aligned} \tag{6}$$

where,

$$\begin{aligned} A_k &= (1 + \Delta_k), \\ B_k &= -\alpha\beta\Delta_k, \\ h &= 1, \\ u &= 1. \end{aligned} \tag{7}$$

The time increment between measurements Δ_k is not constant since measurements were taken at non-uniform sampling rate. This implies that some of the parameters of the model in equation (6) will change through time. Furthermore, v and w are normal random variables with zero mean and Q and R variance respectively. The description of the Kalman filtering algorithm is omitted from this article. A thorough description of the algorithm can be found in Stengel (1994), a description of how the algorithm is used for forecasting can be found in Chatfield (2003) and an example of its usage for prognostics can be found in (Saha et al., 2009).

5.2. Future state forecasting

The use of the Kalman filter as a RUL forecasting algorithm requires the evolution of the state without updating the error covariance matrix and the posterior of the state vector. The n step ahead forecasting equation for the Kalman filter is given below. The last update is done at the time of the last measurement t_l.

$$\hat{x}_{l+n} = A^n x_l + \sum_{i=0}^{n-1} A^i B \tag{8}$$

The subscripts from parameters A and B are omitted since a constant Δ_t is used in the forecasting mode (one prediction every hour).

5.3. Noise models

The model noise variance Q was estimated from the model regression residuals for each test case as presented in table 1. This variance was used for the model noise in the Kalman filter implementation. The measurement noise variance R is also required in the filter implementation. This variance was computed from the direct measurements of the capacitance with the EIS equipment, the observed variance is 4.99×10^{-7}.

6. PREDICTION OF REMAINING USEFUL LIFE RESULTS

Estate estimation and RUL prediction results are discussed for test case $T6$. Figure 11 shows the result of the filter tracking the complete degradation signal. The residuals show an increased error with aging time. This is to be expected given the results observed from the model estimation process.

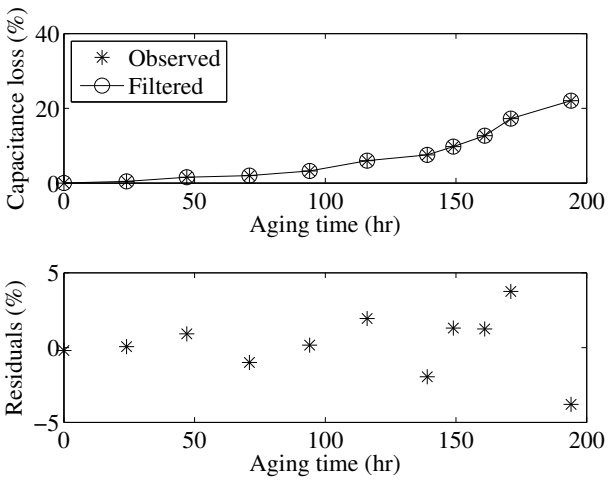

Figure 11. Tracking results for the Kalman filter implementation applied to test capacitor (capacitor #6).

Figure 12 presents results from the remaining useful life prediction algorithm at time $t_p = 161$ (hr), which is the time at which ESR and C measurements are taken. The failure threshold is considered to be a crisp value of 20% decrease in capacitance. End of life (EOL) is defined as the time at which the forecasted percentage capacity loss trajectory crosses the EOL threshold. Therefore, RUL is EOL minus 161 hours.

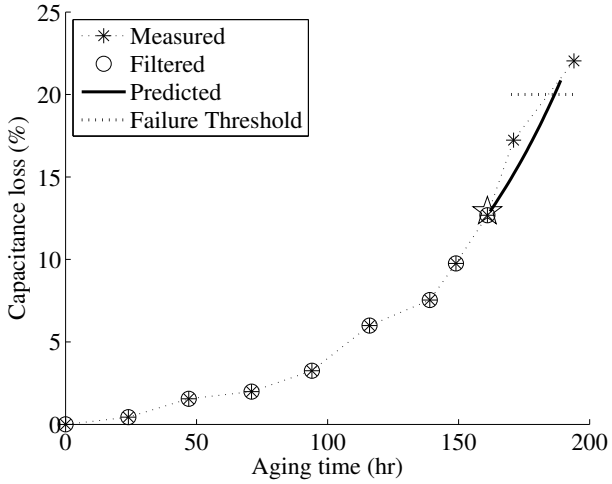

Figure 12. Remaining useful life prediction at time 149 (hr).

Figure 13 presents the capacitance loss estimation and EOL prediction at different points during the aging time. Predic-

tions are made after each point in which measurements are available. It can be observed that the predictions become better as the prediction is made closer to the actual EOL. This is possible because the estimation process has more information to update the estimates as it nears EOL. Figure 14 presents a zoomed-in version of figure 13 focusing in the area close to the failure threshold.

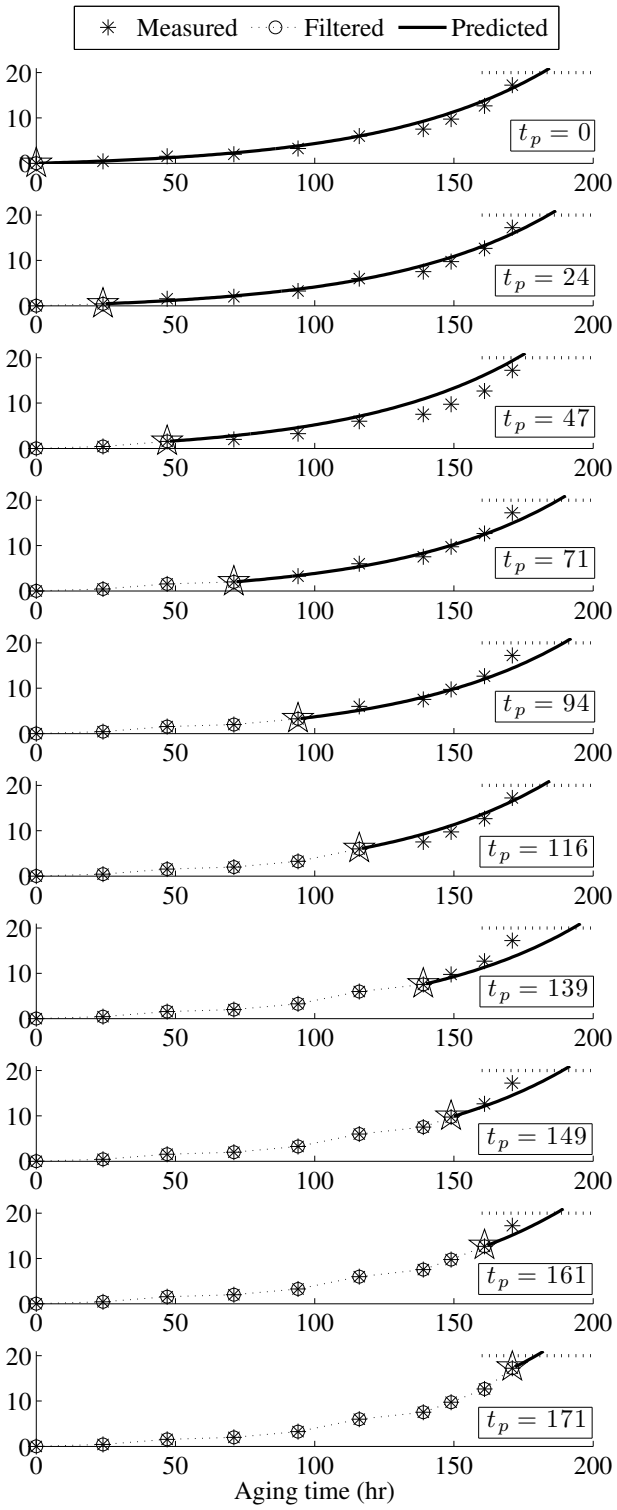

Figure 13. T_6: Health state estimation and forecasting of capacitance loss (%) at different times t_p during the aging time; $t_p = [0, 24, 47, 71, 94, 116, 139, 149, 161, 171]$.

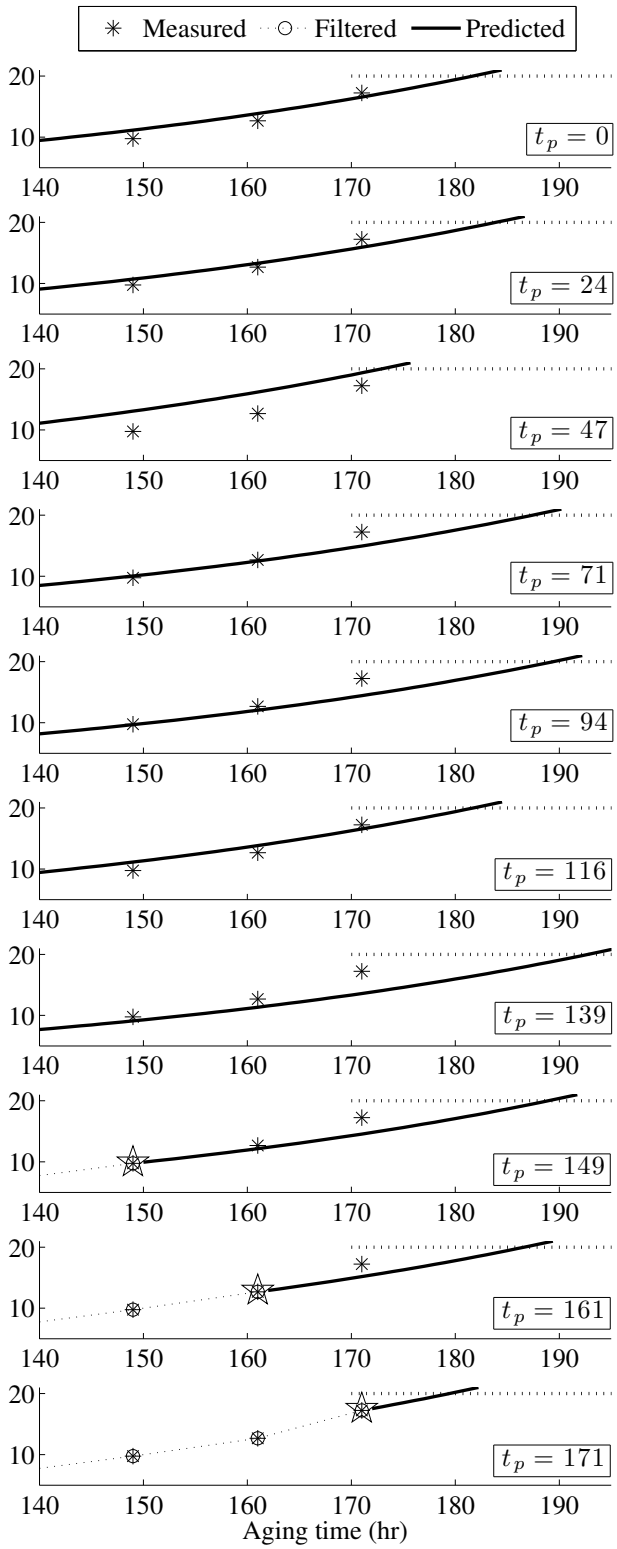

Figure 14. T_6: Detail of the health state estimation and forecasting of capacitance loss (%) at different times t_p during the aging time; $t_p = [0, 24, 47, 71, 94, 116, 139, 149, 161, 171]$.

An α-λ prognostics performance metric is presented in Figure 15 for validation test T_6. The blue line represents ground truth and the shaded region is corresponding to a 30% ($\alpha = 0.3$) error bound in the RUL prediction. This metric specifies that the prediction is within the error bound halfway between first prediction and EOL ($\lambda = 0.5$). In addition, this metric allows us to visualize how the RUL prediction performance changes as data closer to EOL becomes available. Appendix B presents the α-λ metric plots for the remaining validation cases.

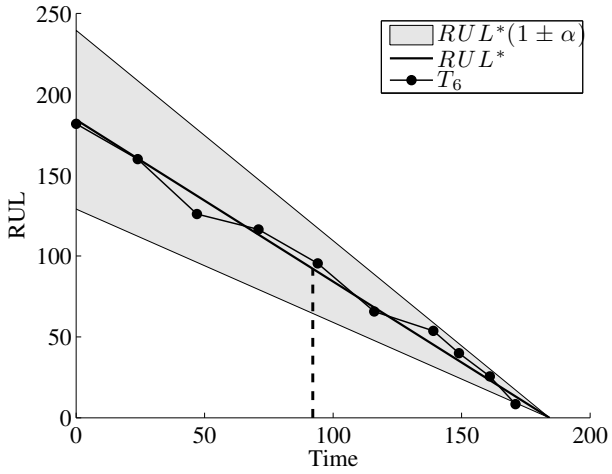

Figure 15. Performance based on α-λ performance metric.

6.1. Validation tests

Table 2 summarizes results for the remaining life prediction at all points in time where measurements are available. The last column indicates the RUL prediction error. The magnitude of the error decreases as the prediction time gets closer to EOL. The decrease is not monotonic which is to be expected when using a tracking framework to estimate health state because the last point of estimation is used to start the forecasting process.

Table 3 shows performance based on the relative accuracy (RA) metric in equation (9). These metrics allows for an assessment of the percentage accuracy relative to the ground-truth value. RA values of 100 represent perfect accuracy. The RA is presented for all the test cases for different prediction times. The last column of the Table 3 represents the median RA of all the test cases for a particular prediction time. It is observed that the RA values decrease considerably for $t_p = 171$. This is consistent with previous observations indicating that the algorithm with a fixed-parameter model is not able to cope with the sudden jump in exponential behavior present around the 171 hour. This is a limitation that could be overcome by either an enhanced degradation model or a an online estimation of degradation model parameters using a more sophisticated Bayesian tracking method like extended

t_p	RUL^*	$RUL^{'}_{T2}$	$RUL^{'}_{T3}$	$RUL^{'}_{T4}$	$RUL^{'}_{T5}$	$RUL^{'}_{T6}$
24	151.04	158.84	164.88	158.76	167.76	159.89
47	128.04	131.32	134.08	128.35	135.32	125.91
71	104.04	117.01	119.88	115.37	122.63	116.41
94	81.04	92.69	96.64	93.09	97.6	95.42
116	59.04	67.28	65.39	67.77	69.5	65.71
139	36.04	44.01	44.72	46.88	49.4	53.75
149	26.04	30.67	32.41	33.55	35.92	39.95
161	14.04	17.23	18.28	18.2	22.64	25.6
171	4.04	1.07	2.89	N/A	5.52	8.45

Table 2. Summary of RUL forecasting results.

Kalman filter or particle filter.

$$RA = 100\left(1 - \frac{RUL^* - RUL^{'}}{RUL^*}\right) \tag{9}$$

t_p	RA_{T2}	RA_{T3}	RA_{T4}	RA_{T5}	RA_{T6}	$\widetilde{RA}$
24	94.8	95.5	91.9	96.9	99.7	**95.5**
47	97.4	99.3	96.4	96.7	91.7	**96.7**
71	87.5	91.9	84.5	94.1	97.1	**91.9**
94	85.6	90	78.9	94.8	94.2	**90**
116	86	99.1	76.5	98	96.2	**96.2**
139	77.8	95.8	53.1	96.7	81.1	**81.1**
149	82.1	98.4	46.9	94.8	86.6	**86.6**
161	77.2	87.3	16.6	87.5	89.8	**87.3**
171	26.6	26.4	N/A	34.8	63.7	**30.7**

Table 3. Validation based on relative accuracy metric.

7. CONCLUSION

This paper presents a RUL prediction algorithm based on accelerated life test data and an empirical degradation model. The main contributions of this work are: a) the identification of the lumped-parameter model (Figure 4) for a real capacitor as a viable reduced-order model for prognostics-algorithm development; b) the identification of the ESR and C model parameters as precursor of failure features; c) the development of an empirical degradation model based on accelerated life test data which accounts for shifts in capacitance as a function of time; d) the implementation of a Bayesian based health state tracking and remaining useful life prediction algorithm based on the Kalman filtering framework. One major contribution of this work is the prediction of remaining useful life for capacitors as new measurements become available.

This capability increases the technology readiness level of prognostics applied to electrolytic capacitors. The results presented here are based on accelerated life test data and on the accelerated life timescale. Further research will focus on development of functional mappings that will translate the accelerated life timescale into real usage conditions time-scale, where the degradation process dynamics will be slower, and subject to several types of stresses. The performance of the proposed exponential-based degradation model is satisfactory for this study based on the quality of the model fit to the experimental data and the RUL prediction performance as compared to ground truth. As part of future work we will also focus on the exploration of additional models based on the physics of the degradation process and larger sample size for aged devices. Additional experiments are currently underway to increase the number of test samples. This will greatly enhance the quality of the model, and guide the exploration of additional degradation-models, where the loading conditions and the environmental conditions are also accounted for towards degradation dynamics.

ACKNOWLEDGMENT

This work was funded by the NASA Aviation Safety Program, SSAT project.

NOMENCLATURE

C_I	Ideal capacitance value for an ideal capacitor
C_R	Real capacitor value for a non-ideal capacitor model
R_E	Equivalent series resistance of the capacitor
$C_l(k)$	Capacitance percentage loss at time t_k
T_i	Validation test on capacitor i
$\mathcal{M}_i$	Nominal model for a component or system
$\mathcal{D}_i$	Degradation model for a capacitor
R_L	Load resistance on electrical overstress system
V_L	Load voltage on electrical overstress system
V_o	Electrical overstress voltage in aging system
Z_I	Ideal capacitor impedance
Z	Capacitor impedance for non-ideal capacitor model $\mathcal{M}_1$

REFERENCES

Bhatti, U., & Ochieng, W. (2007). Failure modes and models for integrated gps/ins systems. *The Journal of Navigation*, *60*, 327.

Celaya, J., Kulkarni, C., Biswas, G., & Goebel, K. (2011a). A model-based prognostics methodology for electrolytic capacitors based on electrical overstress accelerated aging. *Proceedings of Annual Conference of the PHM Society, September 25-29, Montreal, Canada*.

Celaya, J., Kulkarni, C., Biswas, G., & Goebel, K. (2011b, March). Towards prognostics of electrolytic capacitors. In *AIAA 2011 Infotech@Aerospace Conference*. St. Louis, MO.

Celaya, J., Kulkarni, C., Biswas, G., & Goebel, K. (2012). Prognostic and experimental techniques for electrolytic capacitor health monitoring. *The Annual Reliability and Maintainability Symposium (RAMS), January 23-36, Reno, Nevada.*.

Chatfield, C. (2003). *The analysis of time series: An introduction* (6th ed.). Chapman and Hall/CRC.

Goodman, D., Hofmeister, J., & Judkins, J. (2007). Electronic prognostics for switched mode power supplies. *Microelectronics Reliability*, *47*(12), 1902-1906. (doi: DOI: 10.1016/j.microrel.2007.02.021)

Gu, J., Azarian, M. H., & Pecht, M. G. (2008). Failure prognostics of multilayer ceramic capacitors in temperature-humidity-bias conditions. In *Prognostics and health management, 2008. phm 2008. international conference on* (p. 1-7).

IEC. (2007-03). *60384-4-1 fixed capacitors for use in electronic equipment* (Tech. Rep.).

Judkins, J. B., Hofmeister, J., & Vohnout, S. (2007). A prognostic sensor for voltage regulated switch-mode power supplies. In *Aerospace conference, 2007 ieee* (p. 1-8).

Kulkarni, C., Biswas, G., Bharadwaj, R., & Kim, K. (2010). Effects of degradation in dc-dc converters on avionics systems: A model based approach. *Machinery Failure Prevention Technology Conference, MFPT 2010*.

Kulkarni, C., Biswas, G., & Koutsoukos, X. (2009). A prognosis case study for electrolytic capacitor degradation in dc-dc converters. *Annual Conference of the Prognostics and Health Management Soceity, PHM 2009*.

Kulkarni, C., Biswas, G., Koutsoukos, X., Celaya, J., & Goebel, K. (2010). Integrated diagnostic/prognostic experimental setup for capacitor degradation and health monitoring. In *2010 IEEE AUTOTESTCON* (p. 1-7).

Kulkarni, C., Biswas, G., Koutsoukos, X., Goebel, K., & Celaya, J. (2010a). Experimental studies of ageing in electrolytic capacitors. *Annual Conference of the Prognostics and Health Management Soceity*.

Kulkarni, C., Biswas, G., Koutsoukos, X., Goebel, K., & Celaya, J. (2010b). Physics of Failure Models for Capacitor Degradation in DC-DC Converters. *The Maintenance and Reliability Conference, MARCON 2010*.

MIL-C-62F. (2008). General specification for capacitors, fixed, electrolytic.

Nie, L., Azarian, M. H., Keimasi, M., & Pecht, M. (2007). Prognostics of ceramic capacitor temperature-humidity-bias reliability using mahalanobis distance analysis. *Circuit World*, *33*(3), 21 - 28.

Orsagh, R., Brown, D., Roemer, M., Dabnev, T., & Hess, A. (2005). Prognostic health management for avionics system power supplies. In *Aerospace conference, 2005 ieee* (p. 3585-3591).

Saha, B., Goebel, K., & Christophersen, J. (2009). Comparison of prognostic algorithms for estimating remaining useful life of batteries. *Transactions of the Institute of Measurement and Control*, *31*(3-4), 293-308.

Stengel, R. F. (1994). *Optimal control and estimation*. Dover Books on Advanced Mathematics.

José R. Celaya is a research scientist with SGT Inc. at the Prognostics Center of Excellence, NASA Ames Research Center. He received a Ph.D. degree in Decision Sciences and Engineering Systems in 2008, a M. E. degree in Operations Research and Statistics in 2008, a M. S. degree in Electrical Engineering in 2003, all from Rensselaer Polytechnic Institute, Troy New York; and a B. S. in Cybernetics Engineering in 2001 from CETYS University, México.

Chetan S. Kulkarni is a Ph.D candidate at ISIS, Vanderbilt University. He received the M.S. degree in EECS from Vanderbilt University, Nashville, TN, in 2009 and a B. E. in Electronics and Electrical Engineering in 2002 from the University of Pune, India.

Kai Goebel received the degree of Diplom-Ingenieur from the Technische Universitt Mnchen, Germany in 1990. He received the M.S. and Ph.D. from the University of California at Berkeley in 1993 and 1996, respectively. Dr. Goebel is a senior scientist at NASA Ames Research Center where he leads the Diagnostics and Prognostics groups in the Intelligent Systems division. In addition, he directs the Prognostics Center of Excellence and he is the technical lead for Prognostics and Decision Making of NASAs System-wide Safety and Assurance Technologies Program. He worked at General Electrics Corporate Research Center in Niskayuna, NY from 1997 to 2006 as a senior research scientist. He has carried out applied research in the areas of artificial intelligence, soft computing, and information fusion. His research interest lies in advancing these techniques for real time monitoring, diagnostics, and prognostics. He holds 15 patents and has published more than 200 papers in the area of systems health management.

Gautam Biswas received the Ph.D. degree in computer science from Michigan State University, East Lansing. He is a Professor of Computer Science and Computer Engineering in the Department of Electrical Engineering and Computer Sci-

ence, Vanderbilt University, Nashville, TN.

A PROGNOSTICS VALIDATION RESULTS

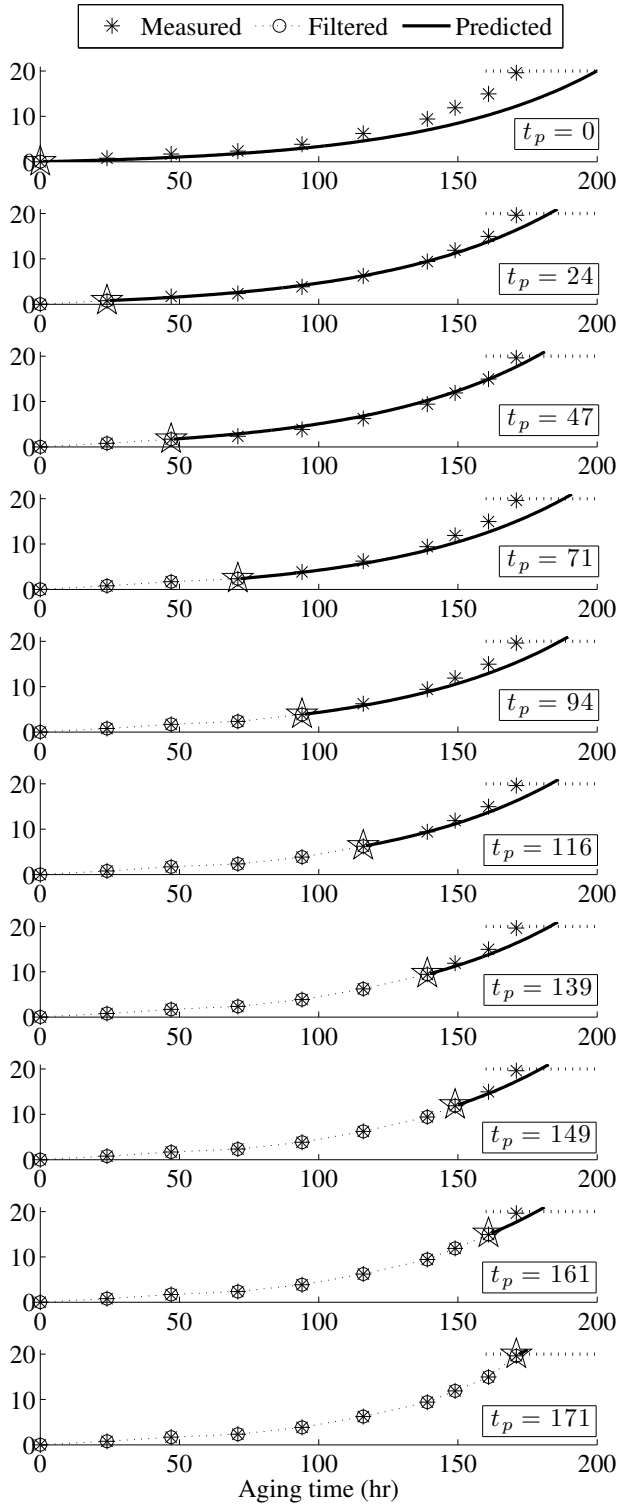

Figure 16. T_2: Health state estimation and forecasting of capacitance loss (%) at different times t_p during the aging time; $t_p = [0, 24, 47, 71, 94, 116, 139, 149, 161, 171]$.

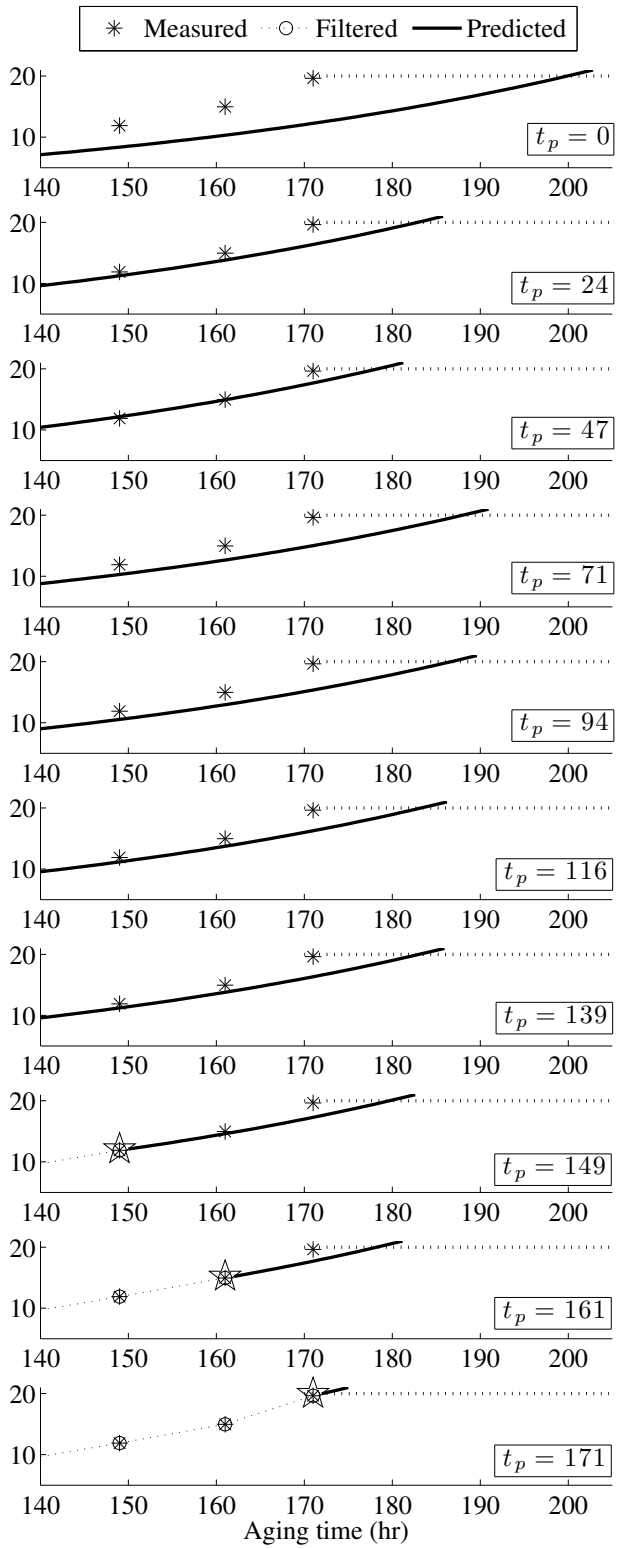

Figure 17. T_2: Detail of the health state estimation and forecasting of capacitance loss (%) at different times t_p during the aging time; $t_p = [0, 24, 47, 71, 94, 116, 139, 149, 161, 171]$.

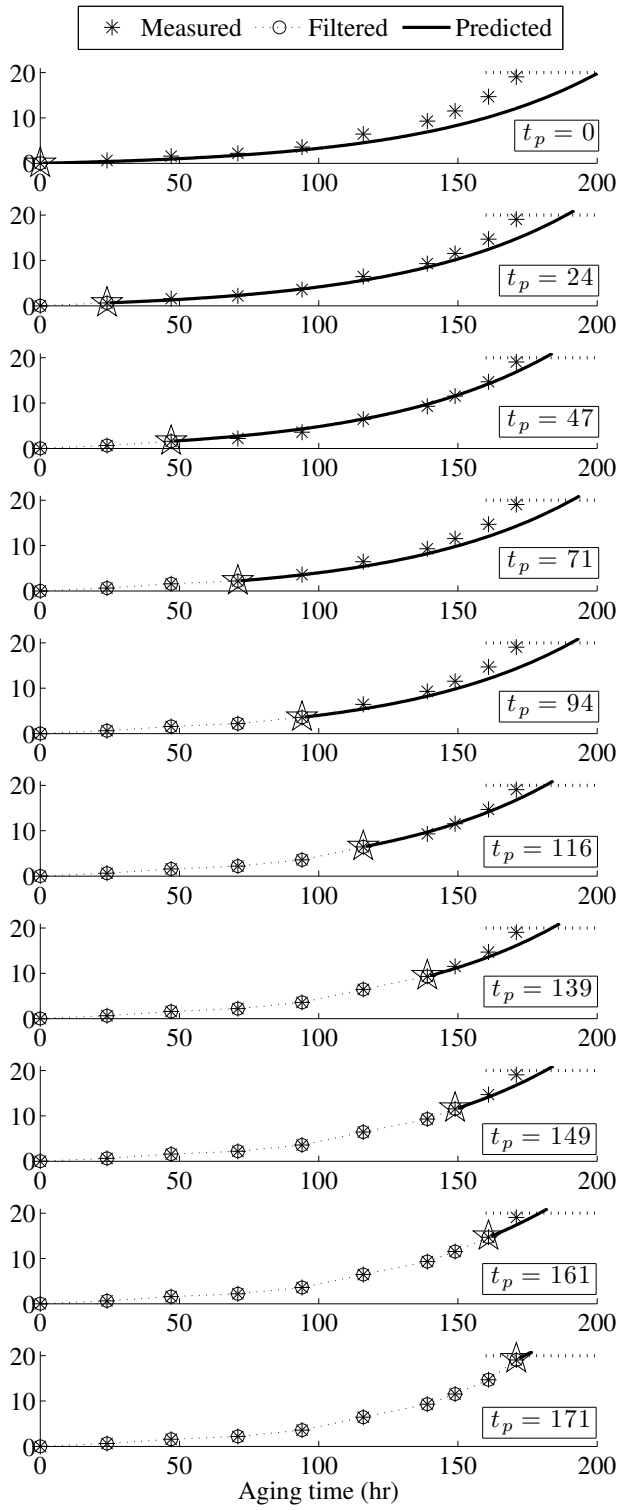

Figure 18. T_3: Health state estimation and forecasting of capacitance loss (%) at different times t_p during the aging time; $t_p = [0, 24, 47, 71, 94, 116, 139, 149, 161, 171]$.

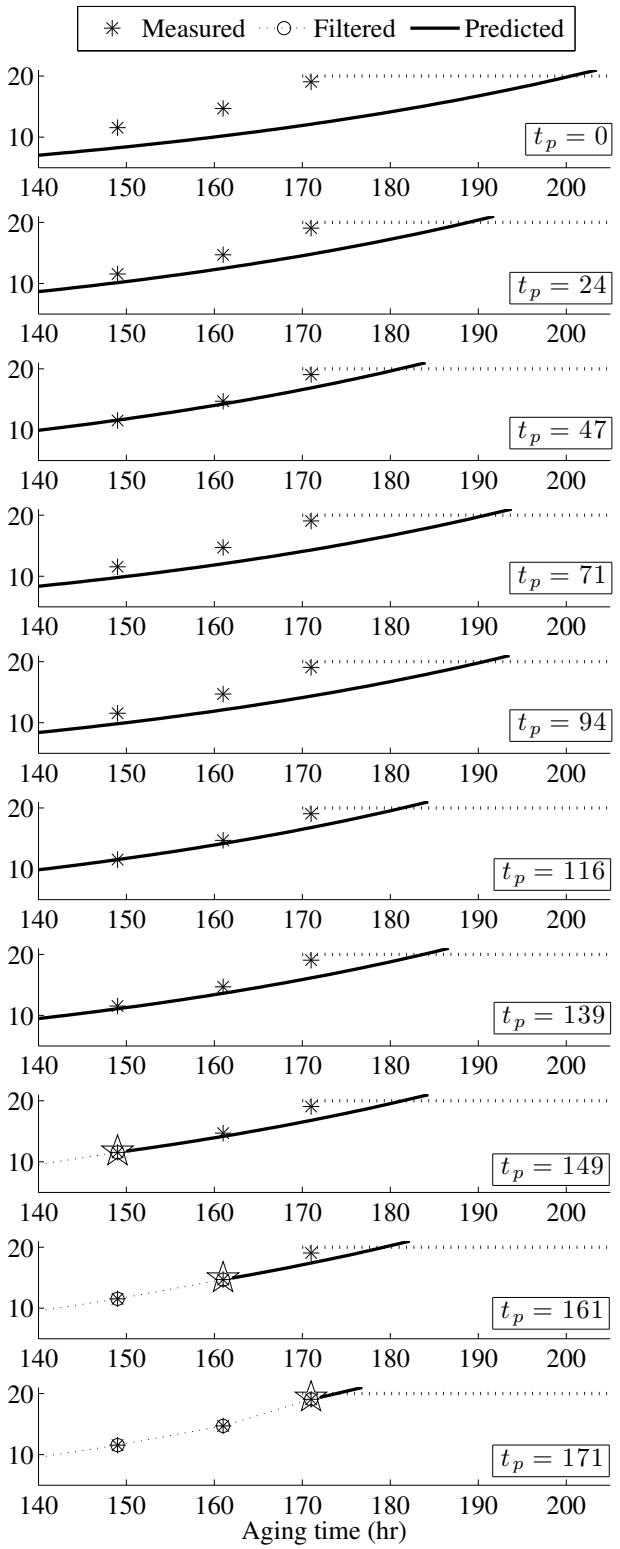

Figure 19. T_3: Detail of the health state estimation and forecasting of capacitance loss (%) at different times t_p during the aging time; $t_p = [0, 24, 47, 71, 94, 116, 139, 149, 161, 171]$.

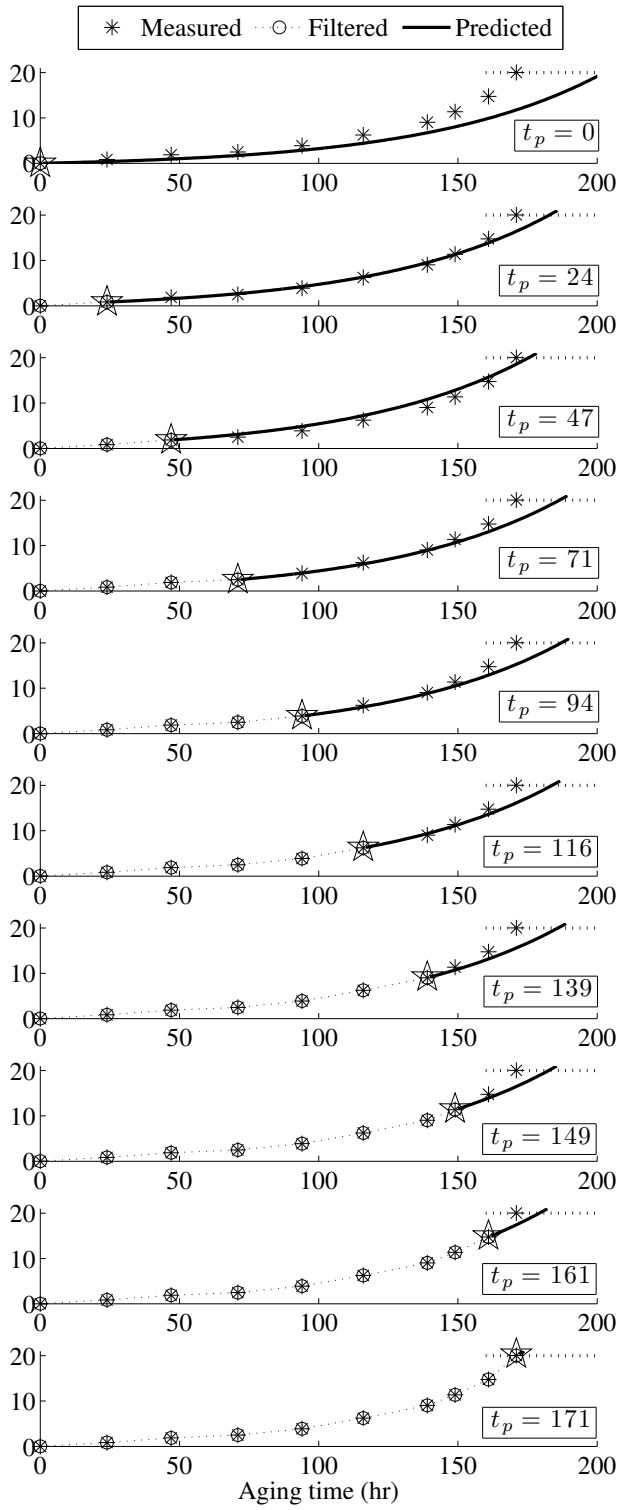

Figure 20. T_4: Health state estimation and forecasting of capacitance loss (%) at different times t_p during the aging time; $t_p = [0, 24, 47, 71, 94, 116, 139, 149, 161, 171]$.

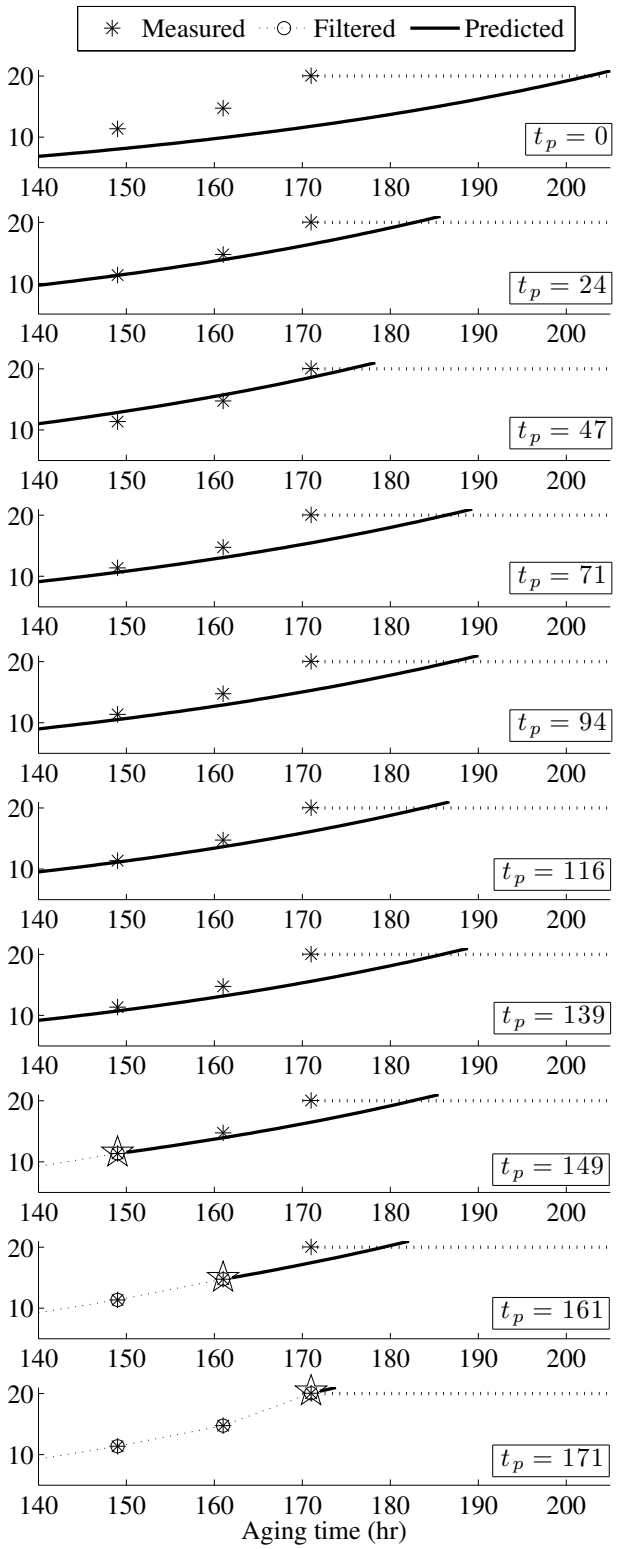

Figure 21. T_4: Detail of the health state estimation and forecasting of capacitance loss (%) at different times t_p during the aging time; $t_p = [0, 24, 47, 71, 94, 116, 139, 149, 161, 171]$.

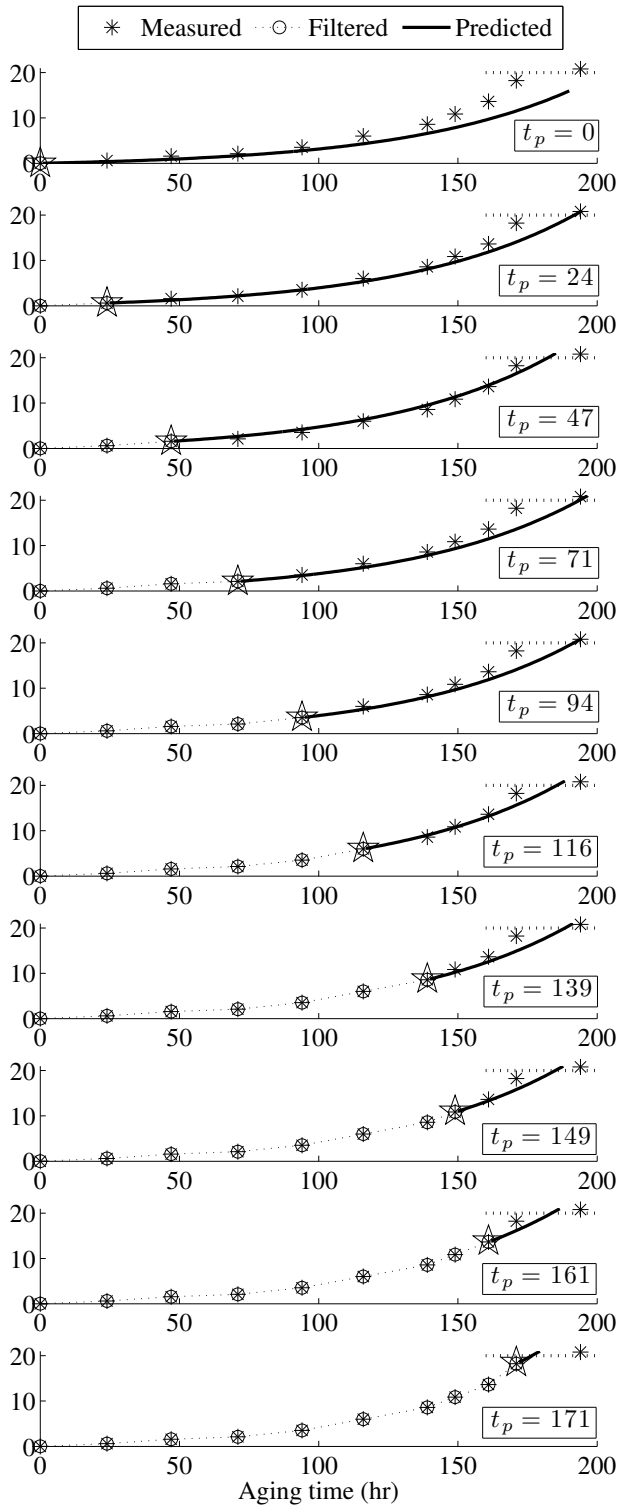

Figure 22. T_5: Health state estimation and forecasting of capacitance loss (%) at different times t_p during the aging time; $t_p = [0, 24, 47, 71, 94, 116, 139, 149, 161, 171]$.

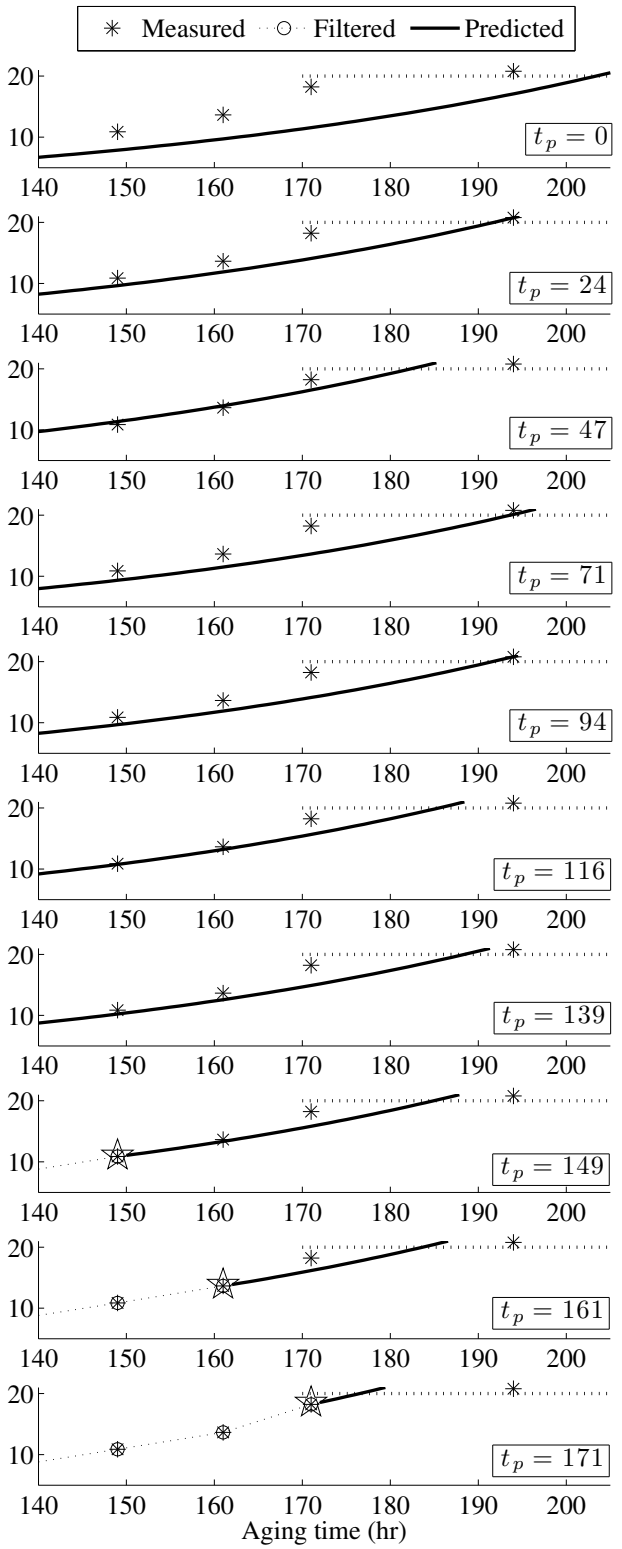

Figure 23. T_5: Detail of the health state estimation and forecasting of capacitance loss (%) at different times t_p during the aging time; $t_p = [0, 24, 47, 71, 94, 116, 139, 149, 161, 171]$.

A PROGNOSTICS ALPHA-LAMBDA PERFORMANCE METRIC

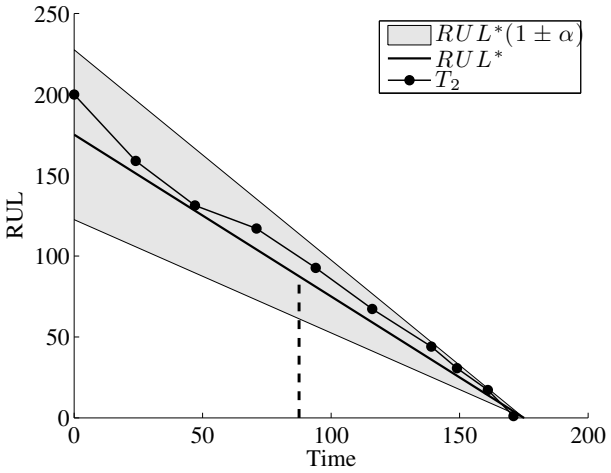

Figure 24. T_2: Alpha-Lambda Prognostics Metric ($\lambda = 0.5$ and $\alpha = 0.3$).

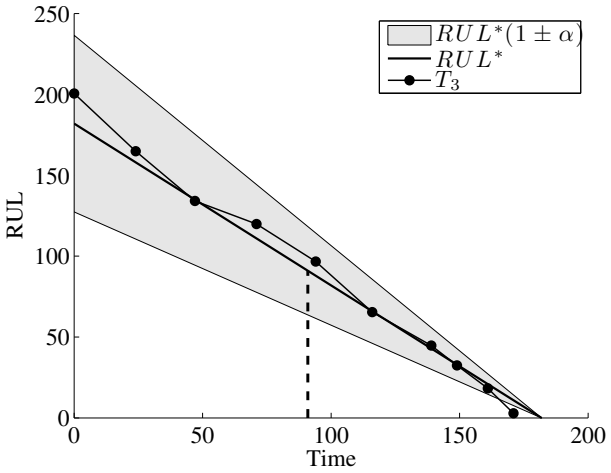

Figure 25. T_3: Alpha-Lambda Prognostics Metric ($\lambda = 0.5$ and $\alpha = 0.3$).

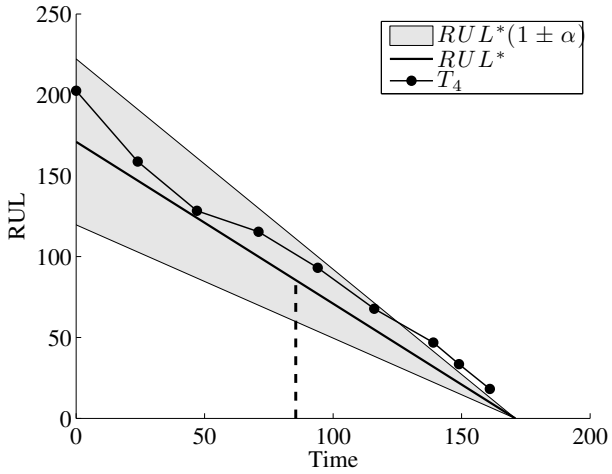

Figure 26. T_5: Alpha-Lambda Prognostics Metric ($\lambda = 0.5$ and $\alpha = 0.3$).

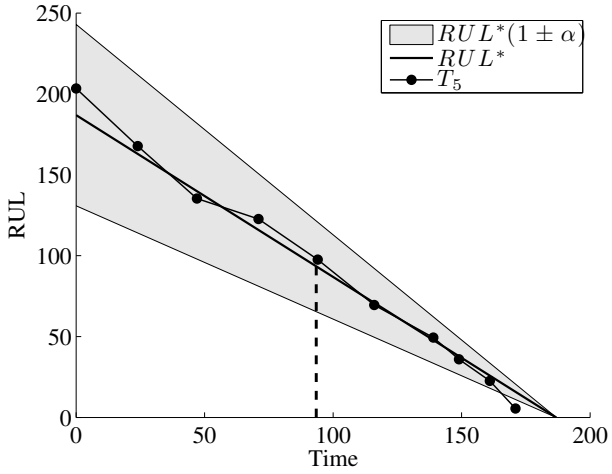

Figure 27. T_5: Alpha-Lambda Prognostics Metric ($\lambda = 0.5$ and $\alpha = 0.3$).

Towards A Model-based Prognostics Methodology for Electrolytic Capacitors: A Case Study Based on Electrical Overstress Accelerated Aging

José R. Celaya[1], Chetan Kulkarni[2], Gautam Biswas[2] and Kai Goebel[3]

[1]SGT Inc., Prognostics Center of Excellence, NASA Ames Research Center
[2]ISIS, Vanderbilt University
[3]Prognostics Center of Excellence, NASA Ames Research Center

Outline

- ~~Motivation and background~~
- Prognostics approach
- Accelerated aging experiments
- Degradation modeling
- Prognostics method and results
- Discussion

Motivation

- Electronic components have increasingly critical role in on-board, autonomous functions for
  - Vehicle controls, communications, navigation, radar systems
- Future aircraft systems will rely more on electronic components
- Assumption of new functionality increases number of electronics faults with perhaps unanticipated fault modes
- We need understanding of behavior of deteriorated components to develop capability to anticipate failures/predict remaining RUL

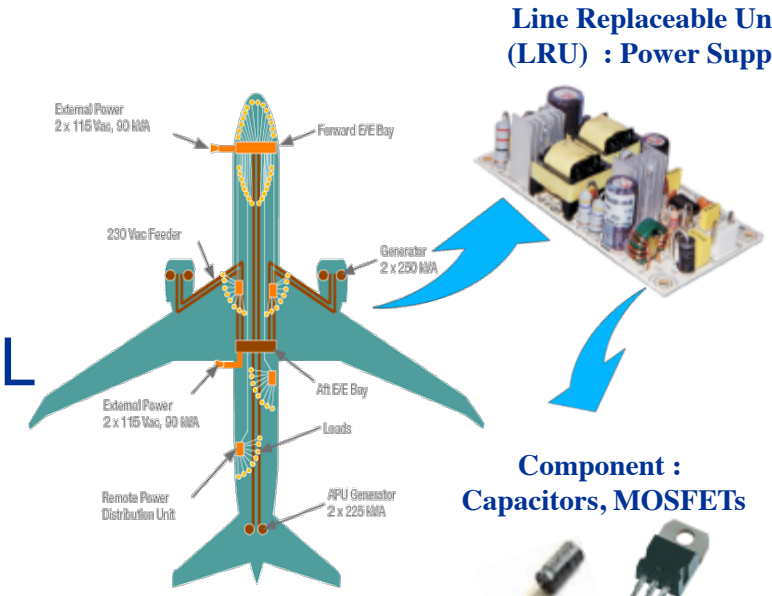

Images courtesy : Boeing

Prognostics Research Approach for Electronics

Model-based prognostics (1/3)

$$\dot{\mathbf{x}}(t) = f(\mathbf{x}(t), u(t)) + w(t)$$
$$y(t) = h(\mathbf{x}(t)), u(t)) + v(k)$$

$$R(t_p) = t_{EOL} - t_p$$

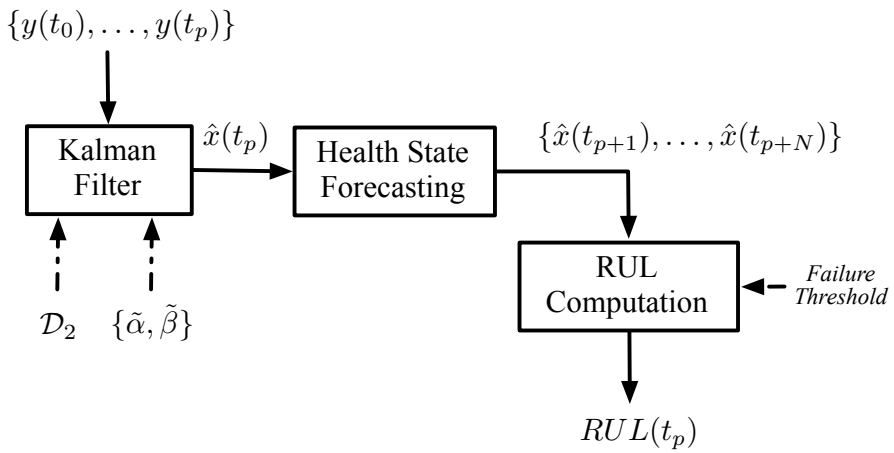

- State vector includes dynamics of the degradation process
- It might include nominal operation dynamics
- EOL defined at time in which performance variable cross failure threshold
- Failure threshold could be crisp or also a random variable

Model-based prognostics (2/3)

- Tracking of health state based on measurements
- Forecasting of health state until failure threshold is crossed
- Compute RUL as function of EOL defined at time failure threshold is crossed

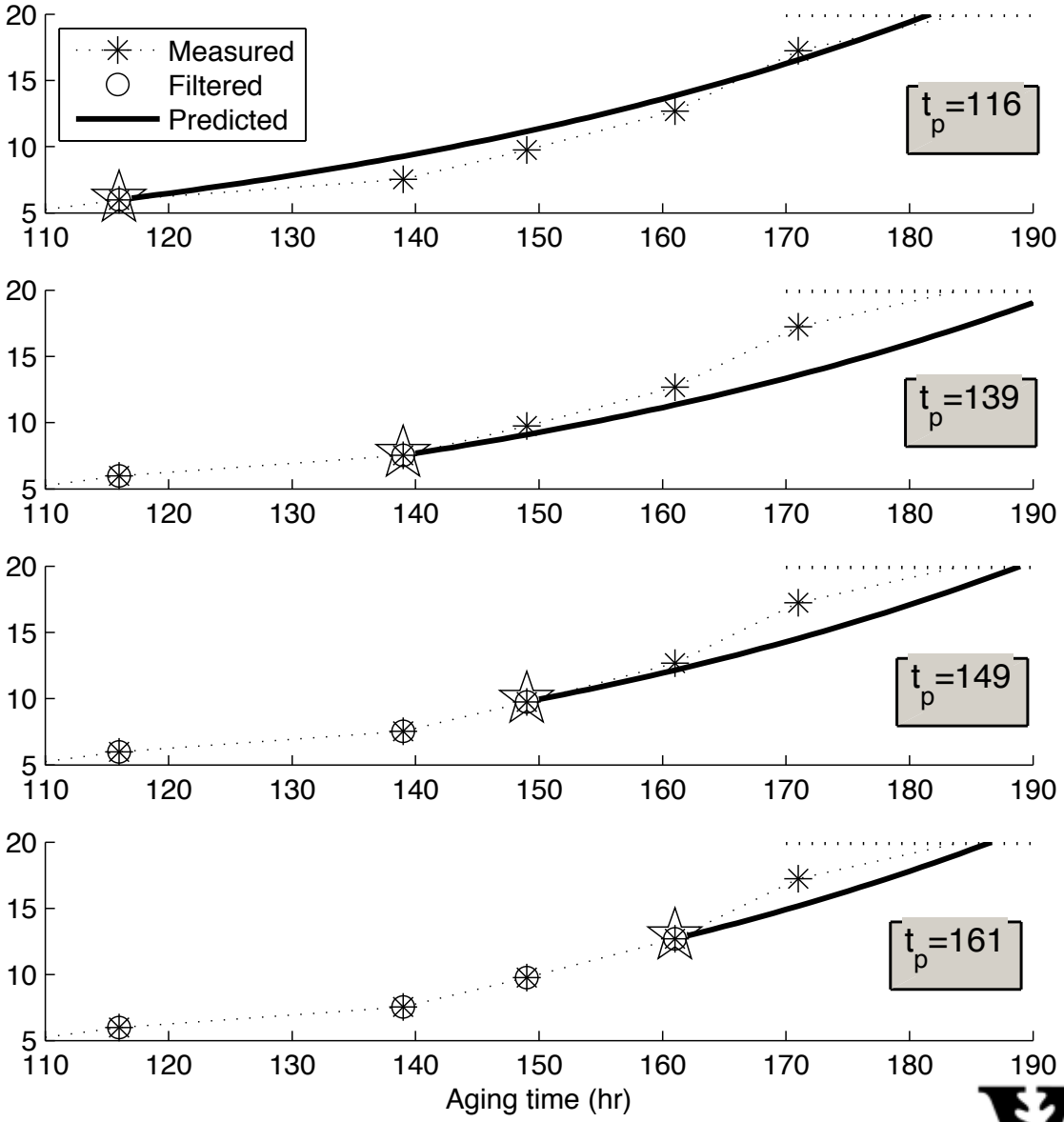

Model-based prognostics (3/3)

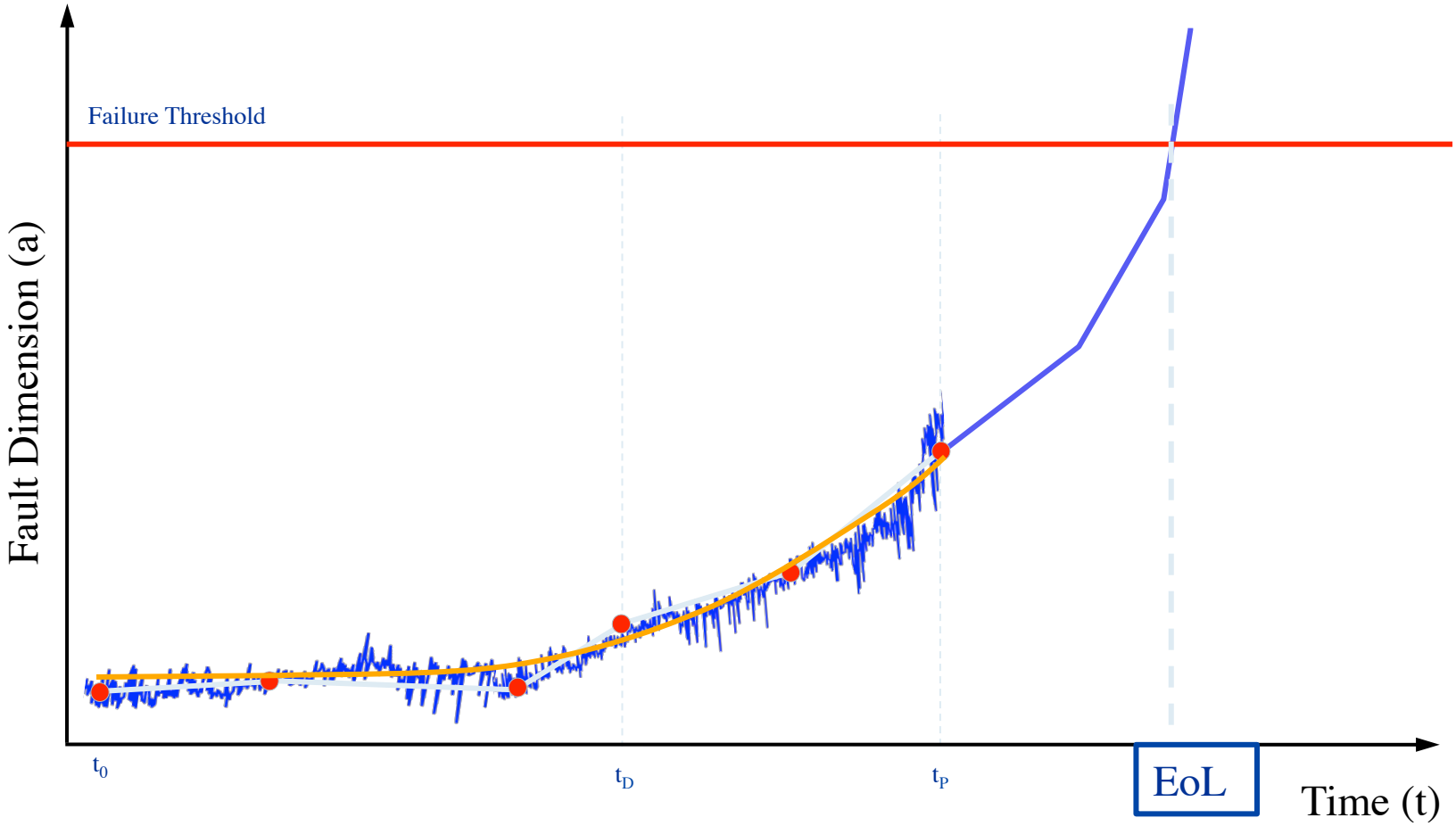

Methodology

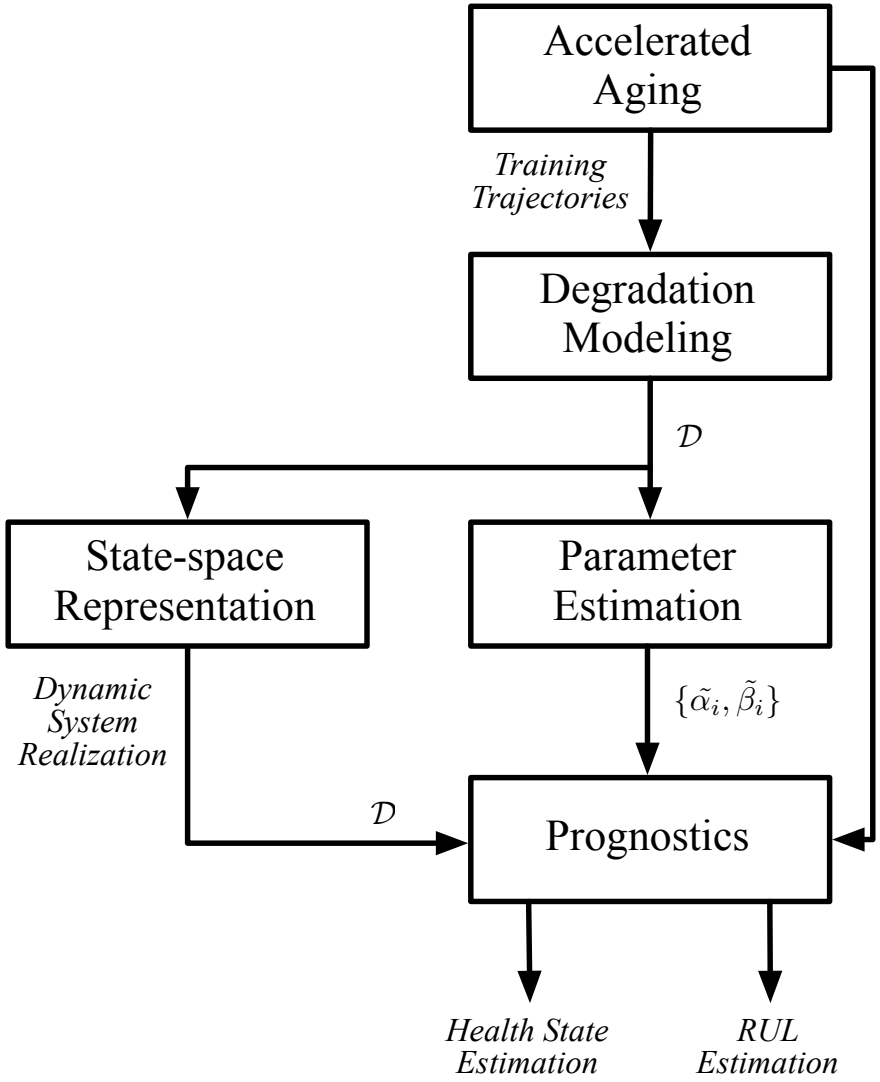

$$x_k = Ax_{k-1} + Bu_{k-1} + w_{k-1}$$

$$y_k = Hx_k + v_k$$

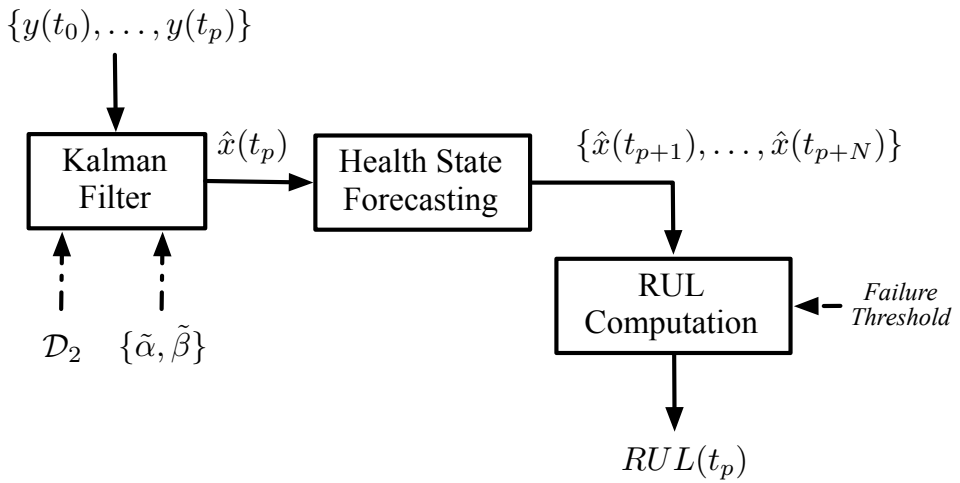

Accelerated Aging Systems for Prognostics

Electrical Overstress Aging System

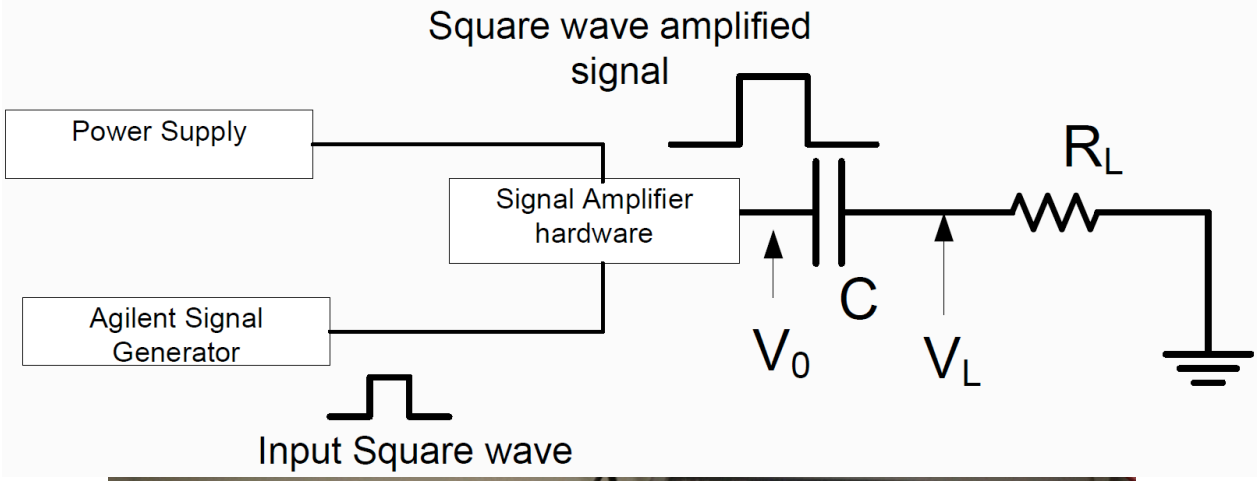

Methodology

Real Capacitor

EIS

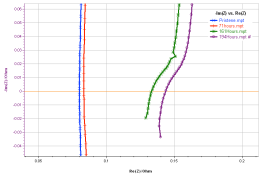

Reduced order model

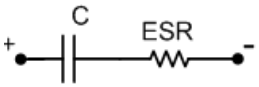

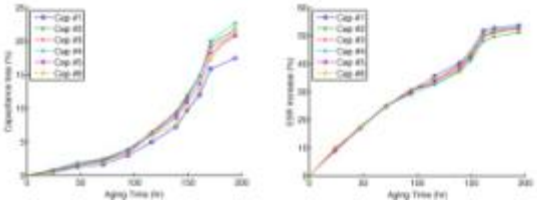

Degradation model (time)

$$C_k = e^{\alpha t_k} + \beta$$

Health state estimation

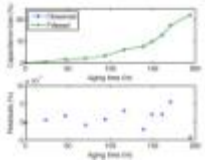

RUL prediction

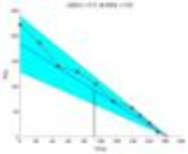

Dynamic modeling of the degradation process

Empirical degradation model

- Based on observed degradation from capacitance parameter
- Using training capacitor data to estimate degradation model parameters
- Assumed exponential model based on capacitance loss
- Parameter estimation with least-squared regression

$$C_k = e^{\alpha t_k} + \beta$$

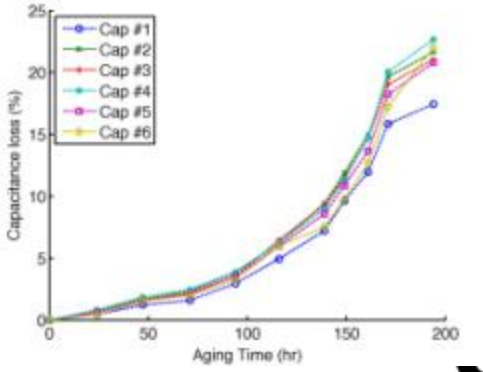

Degradation model results

Validation test	Test capacitor	Training capacitor	α (95% CI)	β (95% CI)	σ_v^2
T_2	#2	#1, #3–#6	**0.0162** (0.0160, 0.0164)	**-0.8398** (-1.1373, -0.5423)	1.8778
T_3	#3	#1, #2, #4–#6	**0.0162** (0.0160, 0.0164)	**-0.8287** (-1.1211, -0.5363)	1.9654
T_4	#4	#1–#3, #5, #6	**0.0161** (0.0159, 0.0162)	**-0.8217** (-1.1125, -0.5308)	1.8860
T_5	#5	#1–#4, #6	**0.0162** (0.0161, 0.0164)	**-0.7847** (-1.1134, -0.4560)	2.1041
T_6	#6	#1–#5	**0.0169** (0.0167, 0.0170)	**-1.0049** (-1.2646, -0.7453)	2.9812

- The optimal parameter presented along the 95% confidence interval.
- The residuals are modeled as a normally distributed random variable with zero mean and variance

Prognostics method and results

Prognostics algorithm

- Implementation of prognostics algorithm with Kalman filter
- Capacitance loss considered as state variable
- EIS measurements and lumped parameter model used to obtained measured capacitance loss values
- Empirical degradation model used to generate the state transition equation
- Use one Capacitor for testing and the rest for model parameter estimation (leave on out test)
- Failure threshold of 20% drop on capacitance based on MIL-C-62F

Kalman filter implementation

- State transition equation derived from degradation model

$$C_k = e^{\alpha t_k} + \beta$$

$$\frac{\partial C}{\partial t} = \alpha C - \alpha\beta$$

$$\frac{C_t - C_{t-\Delta t}}{\Delta t} = \alpha C_{t-\Delta t} - \alpha\beta$$

$$C_t = (1 + \alpha\Delta_t)C_{t-\Delta t} - \alpha\beta\Delta_t$$

$$C_k = (1 + \alpha\Delta_k)C_{k-1} - \alpha\beta\Delta_k$$

- State-space model for filter implementation

$$C_k = A_k C_{k-1} + B_k u + v$$

$$y_k = hC_k + w, \text{where}$$

$$A_k = (1 + \Delta_t),$$

$$B_k = -\alpha\beta\Delta_k,$$

$$h = 1,\ u = 1.$$

Prediction mode

- Assumed measurements are not available at some point in time
- Filter used in forecasting mode to predict future states
- Predictions done at 1 hr. intervals
- State transition equation used to propagate state (n: number of prediction steps, *l*: last measurement at t_l)

$$\hat{C}_{l+n} = A^n C_l + \sum_{i=0}^{n-1} A^i B$$

Tracking and forecasting (Cap. #6)

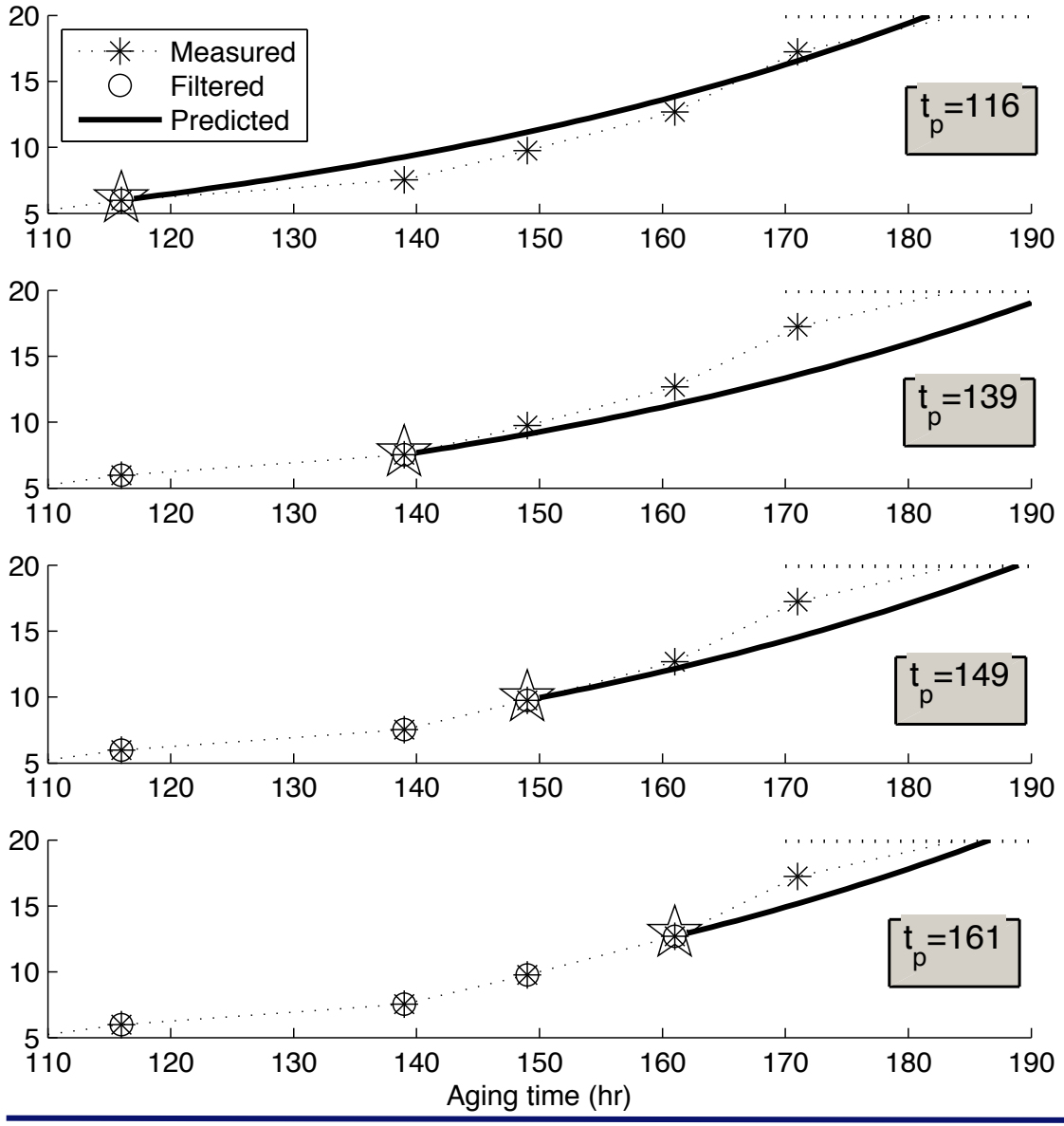

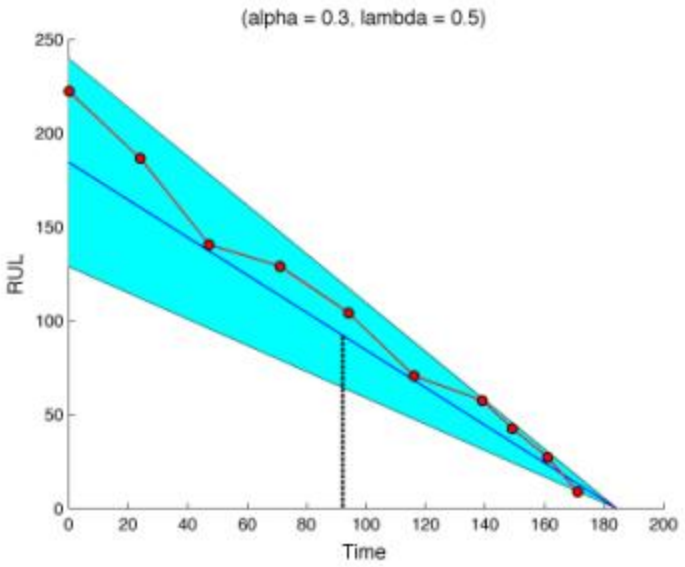

Relative Accuracy

$$RA = 100\left(1 - \frac{RUL^* - RUL'}{RUL^*}\right)$$

t_p	RA_{T2}	RA_{T3}	RA_{T4}	RA_{T5}	RA_{T6}	$\widetilde{RA}$
24	94.8	95.5	91.9	96.9	99.7	**95.5**
47	97.4	99.3	96.4	96.7	91.7	**96.7**
71	87.5	91.9	84.5	94.1	97.1	**91.9**
94	85.6	90	78.9	94.8	94.2	**90**
116	86	99.1	76.5	98	96.2	**96.2**
139	77.8	95.8	53.1	96.7	81.1	**81.1**
149	82.1	98.4	46.9	94.8	86.6	**86.6**
161	77.2	87.3	16.6	87.5	89.8	**87.3**
171	26.6	26.4	N/A	34.8	63.7	**30.7**

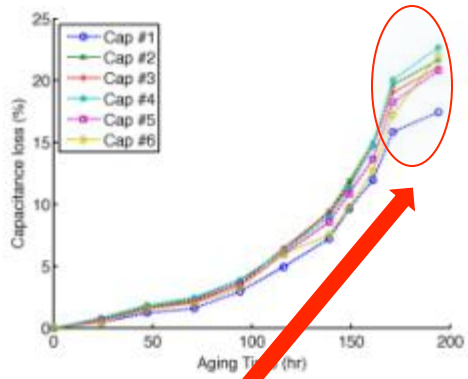

Discussion

Contribution

- RUL prediction algorithm based on accelerated life test data and an empirical degradation model
  - Identification of the lumped-parameter model for a real capacitor as a viable reduced-order model for prognostics-algorithm development
  - Identification of ESR and C as precursor of failure feature parameters
  - Development of an empirical degradation model based on accelerated life test data which accounts for shifts in capacitance as a function of time
  - Implementation of a Bayesian based health state tracking and RUL prediction algorithm based on the Kalman filtering framework

Comments

- Proposed approach requires further development
  - Results presented over accelerated aging test time scale
  - The empirical degradation model can be improved.
  - Degradation model and prediction algorithm assume constant loading and environmental conditions
  - Explore more sophisticated Bayesian tracking algorithms if required to handle variable loading and operational conditions as well as degradation models with time varying parameters
  - Uncertainty representation in the forecasting section and model uncertainty assessment under the Bayesian tracking framework

Thank You

This work was funded by NASA, Aviation Safety Program, IVHM and SSAT Projects

Backup slides

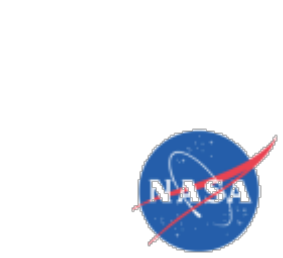

Results (all)

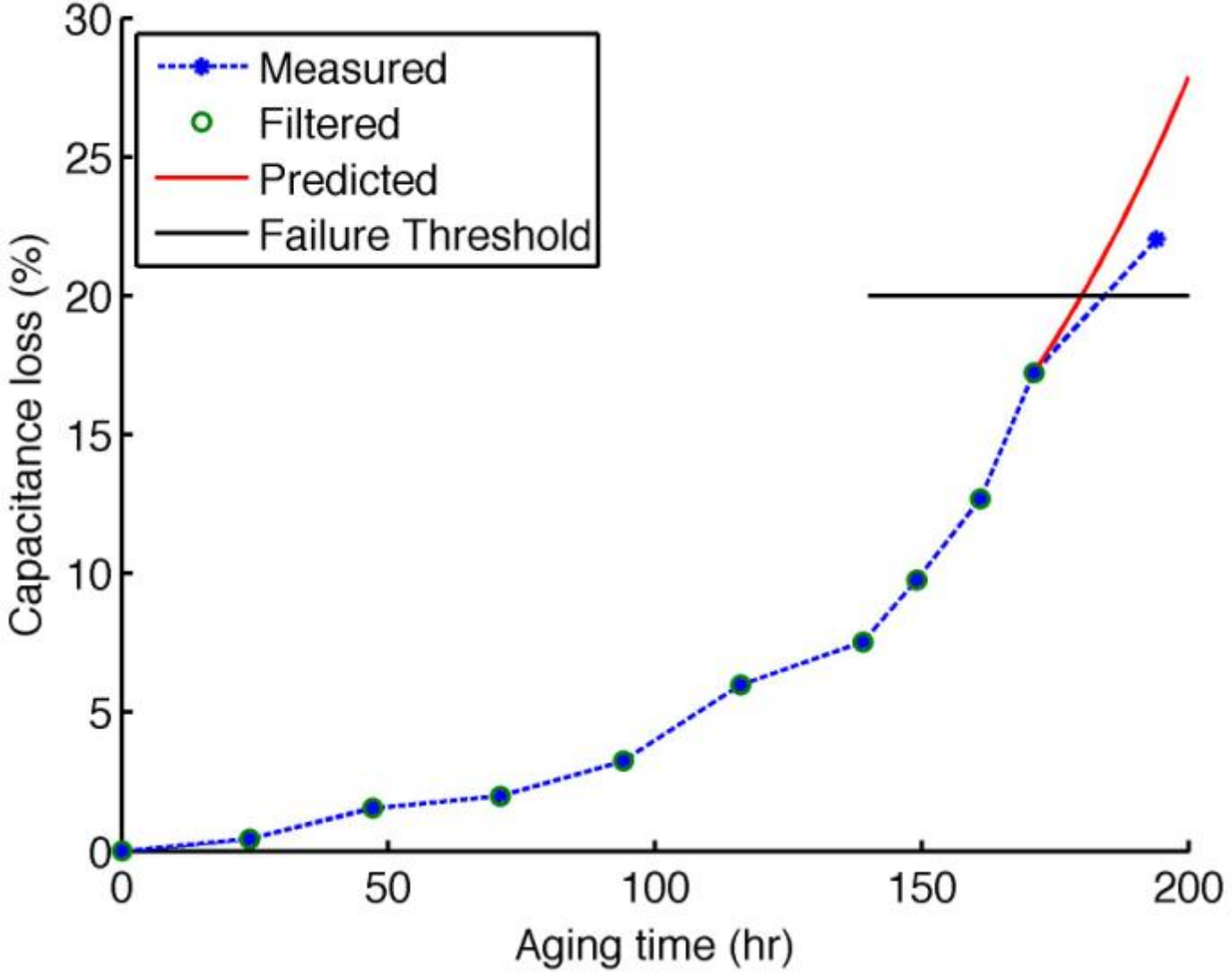
Measured
Filtered
Predicted
Failure Threshold
Capacitance loss (%)
Aging time (hr)
0
5
10
15
20
25
30
0
50
100
150
200

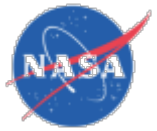

RUL Results for all test cases

t_p	RUL^*	RUL'_{T2}	RUL'_{T3}	RUL'_{T4}	RUL'_{T5}	RUL'_{T6}
24	151.04	158.84	164.88	158.76	167.76	159.89
47	128.04	131.32	134.08	128.35	135.32	125.91
71	104.04	117.01	119.88	115.37	122.63	116.41
94	81.04	92.69	96.64	93.09	97.6	95.42
116	59.04	67.28	65.39	67.77	69.5	65.71
139	36.04	44.01	44.72	46.88	49.4	53.75
149	26.04	30.67	32.41	33.55	35.92	39.95
161	14.04	17.23	18.28	18.2	22.64	25.6
171	4.04	1.07	2.89	N/A	5.52	8.45

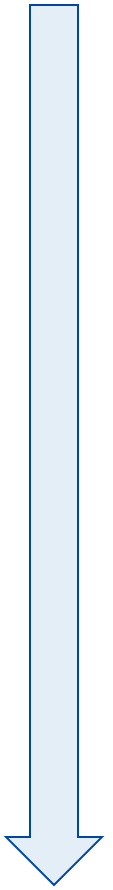

Degradation on lumped parameter model

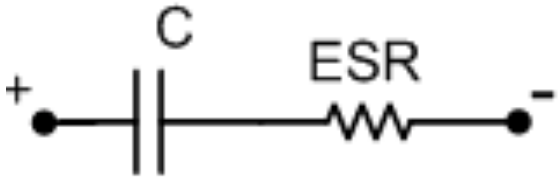

C and ESR are estimated from EIS measurements